

Weakly-Interacting Massive Particles in Non-supersymmetric SO(10) Grand Unified Models

Natsumi Nagata^{a,b}, Keith A. Olive^a, and Jiaming Zheng^a

^a*William I. Fine Theoretical Physics Institute, School of Physics and Astronomy,
University of Minnesota, Minneapolis, MN 55455, USA*

^b*Kavli IPMU (WPI), UTIAS, University of Tokyo, Kashiwa, Chiba 277-8583, Japan*

Abstract

Non-supersymmetric SO(10) grand unified theories provide a framework in which the stability of dark matter is explained while gauge coupling unification is realized. In this work, we systematically study this possibility by classifying weakly interacting dark matter candidates in terms of their quantum numbers of $SU(2)_L \otimes U(1)_Y$, $B-L$, and $SU(2)_R$. We consider both scalar and fermion candidates. We show that the requirement of a sufficiently high unification scale to ensure a proton lifetime compatible with experimental constraints plays a strong role in selecting viable candidates. Among the scalar candidates originating from either a **16** or **144** of SO(10), only $SU(2)_L$ singlets with zero hypercharge or doublets with $Y = 1/2$ satisfy all constraints for $SU(4)_C \otimes SU(2)_L \otimes SU(2)_R$ and $SU(3)_C \otimes SU(2)_L \otimes SU(2)_R \otimes U(1)_{B-L}$ intermediate scale gauge groups. Among fermion triplets with zero hypercharge, only a triplet in the **45** with intermediate group $SU(4)_C \otimes SU(2)_L \otimes SU(2)_R$ leads to solutions with $M_{\text{GUT}} > M_{\text{int}}$ and a long proton lifetime. We find three models with weak doublets and $Y = 1/2$ as dark matter candidates for the $SU(4)_C \otimes SU(2)_L \otimes SU(2)_R$ and $SU(4)_C \otimes SU(2)_L \otimes U(1)_R$ intermediate scale gauge groups assuming a minimal Higgs content. We also discuss how these models may be tested at accelerators and in dark matter detection experiments.

1 Introduction

Various cosmological observations have now established that more than 80% of the energy density of matter in the Universe is composed of non-baryonic dark matter (DM) [1]. The Standard Model (SM) of particle physics, however, cannot explain this observation, and therefore there should be new physics beyond the SM which contains a DM candidate. One of the most promising class of candidates for DM is the so-called weakly-interacting massive particle (WIMP). These are electrically neutral and colorless particles which have masses of $\mathcal{O}(10^{(2-3)})$ GeV and couple to SM particles via weak-scale interactions. Their thermal relic abundance can explain the current energy density of DM. Such particles are predicted in many new-physics models; for example, the lightest neutralino in the supersymmetric (SUSY) SM is a well-known candidate for WIMP DM [2].

For a WIMP to be DM, it should be stable or have a sufficiently long lifetime compared to the age of the Universe. To assure that, it is usually assumed that there is a symmetry which stabilizes the DM particle. For instance, in the minimal SUSY SM (MSSM), R -parity makes the lightest SUSY particle stable and thus a candidate for DM in the Universe [2]. Similarly, Kaluza-Klein parity in universal extra dimensional models [3] and T -parity in the Littlest Higgs model [4] yield stable particles, which can also be promising DM candidates. The ultraviolet (UV) origin of such a symmetry is, however, often obscure; thus it would be quite interesting if a theory which offers a DM candidate and simultaneously explains its stability can be realized as a UV completion rather than introducing the additional symmetry by hand.

In fact, grand unified theories (GUTs) can provide such a framework. Suppose that the rank of a GUT gauge group is larger than four. In this case, the GUT symmetry contains extra symmetries beyond the SM gauge symmetry. These extra symmetries should be spontaneously broken at a high-energy scale by a vacuum expectation value (VEV) of a Higgs field. Then, if we choose the proper representation for the Higgs field, there remains discrete symmetries, which can be used for DM stabilization [5–10]. The discrete charge of each representation is uniquely determined, and thus we can systematically identify possible DM candidates for each symmetry.

In this work, we discuss the concrete realization of this scenario in non-SUSY $SO(10)$ GUT models. It is widely known that $SO(10)$ GUTs [11–13] have a lot of attractive features. Firstly, all of the SM quarks and leptons, as well as right-handed neutrinos, can be embedded into **16** representations of $SO(10)$. Secondly, the anomaly cancellation in the SM is naturally explained since $SO(10)$ is free from anomalies. Thirdly, one obtains improved gauge coupling unification [13–20] and improved fermion mass ratios [13, 21] if partial unification is achieved at an intermediate mass scale. In addition, since right-handed neutrinos have masses of the order of the intermediate scale, small neutrino masses can be explained via the seesaw mechanism [22] if the intermediate scale is sufficiently high. $SO(10)$ includes an additional $U(1)$ symmetry, which is assumed to be broken at the intermediate scale. If the Higgs field that breaks this additional $U(1)$ symmetry belongs to a **126** dimensional representation, then a discrete \mathbb{Z}_2 symmetry is preserved at low energies. One also finds that as long as we focus on relatively small representations

($\leq \mathbf{210}$), the $\mathbf{126}$ Higgs field leaving a \mathbb{Z}_2 symmetry is the only possibility for a discrete symmetry [23, 24]. We focus on this case in the following discussion.

DM candidates appearing in such models can be classified into two types; one class of DM particles have effectively weak-scale interactions with the SM particles so that they are thermalized in the early universe, while the other class contains SM singlets which are never brought into thermal equilibrium. In the latter case, DM particles are produced out of equilibrium via the thermal scattering involving heavy (intermediate scale) particle exchange processes. This type of DM is called Non-Equilibrium Thermal DM (NETDM) [25], whose realization in SO(10) GUTs was thoroughly discussed in Ref. [24]. NETDM is necessarily fermionic as scalar DM would naturally couple to the SM Higgs bosons. Depending on the choice of the intermediate-scale gauge group, candidates for NETDM may originate from several different SO(10) representations such as $\mathbf{45}$, $\mathbf{54}$, $\mathbf{126}$ or $\mathbf{210}$. Although the NETDM candidate itself does not affect the running of the gauge couplings from the weak scale to the intermediate scale, part of the original SO(10) multiplet has a mass at the intermediate scale and does affect the running up to the GUT scale. Demanding gauge coupling unification with a GUT scale above 10^{15} GeV leaves us with a limited set of potential NETDM candidates. When we further demand the splitting of the GUT scale or intermediate scale multiplets so that only a singlet survives at low energies only two candidates were left: in $SU(4)_C \otimes SU(2)_L \otimes SU(2)_R$ notations there were the Dirac $(\mathbf{1}, \mathbf{1}, \mathbf{3})$ originating in a $\mathbf{45}$ or a Weyl $(\mathbf{15}, \mathbf{1}, \mathbf{1})$ also originating from a $\mathbf{45}$ or a $\mathbf{210}$ in SO(10).

In this paper, we study the remaining possibility, namely, that of WIMP DM candidates in SO(10) GUT models. We systematically classify WIMP DM candidates in terms of their quantum numbers and embed them in SO(10) representations. As noted above and discussed in Ref. [24], the presence of DM multiplets significantly affects the running of the gauge coupling constants. In this case, since the DM candidates are no longer SM singlets, the running of the gauge couplings is also affected between the weak and intermediate scales and may spoil gauge coupling unification realized in non-SUSY SO(10) GUTs. We list WIMP DM models in which gauge coupling unification is achieved with appropriate GUT and intermediate scales. Then, we study the phenomenology of these models, such as the relic abundance of DM, the DM direct detection rate, the proton decay lifetime, and neutrino masses. It is found that the condition of gauge coupling unification, as well as the proton decay bounds, severely restricts the WIMP DM models in SO(10) GUTs. Still, we obtain some promising candidates, which can be probed in future DM searches and proton decay experiments.

This paper is organized as follows. In the next section, we show the model setup for the SO(10) WIMP DM scenario. The realization of a \mathbb{Z}_2 symmetry and the classification of WIMP DM candidates are discussed there. Then, we analyze the scalar and fermionic DM models in Sec. 3 and Sec. 4, respectively. Section 5 is devoted to conclusion and discussion.

2 Model

We begin with an overview of the basic SO(10) model needed to accommodate a DM candidate. As mentioned above, in this work, we consider SO(10) GUT models and restrict ourselves to a two step simultaneous symmetry breaking chain,¹ in which the SO(10) gauge group is broken to an intermediate gauge group G_{int} at the GUT scale M_{GUT} , and subsequently broken to the SM gauge group $G_{\text{SM}} \equiv \text{SU}(3)_C \otimes \text{SU}(2)_L \otimes \text{U}(1)_Y$ and a \mathbb{Z}_2 symmetry at the intermediate scale M_{int} :

$$\text{SO}(10) \longrightarrow G_{\text{int}} \longrightarrow G_{\text{SM}} \otimes \mathbb{Z}_2 , \quad (1)$$

The Higgs multiplets that break SO(10) and G_{int} are labeled by R_1 and R_2 , respectively. As discussed in the introduction, this \mathbb{Z}_2 symmetry is a remnant of an extra U(1) symmetry in SO(10) [5–8] and is used to stabilize DM candidates [9, 10]. A brief introduction to the intermediate subgroups and \mathbb{Z}_2 symmetry will be given in Sec. 2.1. Possible SO(10) multiplets that contain an electric and color neutral component for a WIMP DM candidate are summarized in Sec. 2.2. For a group theoretical argument on the classification of these DM candidates, see Appendix A. Among them, those who have a non-zero hypercharge are severely restricted by the DM direct search experiments. We consider this class of DM candidates in Sec. 2.3 and discuss conditions for the DM models to evade the direct search bound.

To keep our model concise, in the following discussion, we only consider SO(10) irreducible representations with dimensions up to 210.

2.1 SO(10) GUT and discrete symmetry

We start by giving a brief description of the ingredients in our model. In an SO(10) unification theory, a generation of SM fermions and a right-handed neutrino are embedded in a **16** chiral representation, while the SM Higgs boson usually lies in a **10** representation. To obtain a realistic Yukawa sector, it is necessary to take the **10** to be complex [27, 28]. We will keep this sector unchanged in most of what follows. In addition to the SM particles, the R_1 and R_2 Higgs representations are added to break SO(10) and G_{int} , respectively. The last ingredient of our model is the DM multiplet, whose lightest component is targeted to be the DM in the Universe. The stability of the DM is guaranteed by a remnant \mathbb{Z}_2 symmetry of the extra U(1) gauge symmetry of SO(10) as we will discuss soon. Possible representations for the DM multiplet are determined below. Here, we assume that only a minimal set of the Higgs and DM multiplets which are necessary for the symmetry breaking and mass generation of DM lie in the low-energy regime and other components have masses of the order of the symmetry breaking scale at which their masses are generated. For example, among the **10** representation, only the electroweak doublet components remains light to break the electroweak symmetry, while the other components have GUT-scale masses. Also, to obtain the right relic abundance, the mass of the DM particle is

¹For recent work on this kind of SO(10) scenario, see Ref. [26].

taken to be of order the TeV scale, while the masses of the other components are either of $\mathcal{O}(M_{\text{GUT}})$ or $\mathcal{O}(M_{\text{int}})$. Such a hierarchical mass spectrum is obtained with fine-tunings similar to the doublet-triplet splitting needed for the **10**. In principle, it may be possible to achieve the splitting of the DM multiplets with a more elaborate scheme of particle representations as in the Higgs doublet-triplet separation [29–31].

SO(10) is a rank-five group so it contains an additional U(1) symmetry besides the SM gauge symmetry. This additional U(1) can be broken into a \mathbb{Z}_2 symmetry by a VEV of an appropriate Higgs field. If we restrict our attention to representation of dimension **210** or less, the only choice of an irreducible R_2 that ensures the \mathbb{Z}_2 symmetry is a **126**.² This \mathbb{Z}_2 symmetry is equivalent to matter parity $P_M = (-1)^{3(B-L)}$ [32], under which the SM fermions are odd, while the SM Higgs field is even. Thus a fermion (boson) is stable if it has an even (odd) matter parity.

We list in Table 1 all possible rank-five subgroups and corresponding R_1 whose VEV breaks SO(10) to the subgroups. Here D denotes the so-called D -parity [33], that is, a \mathbb{Z}_2 symmetry with respect to the exchange of $\text{SU}(2)_L \leftrightarrow \text{SU}(2)_R$. D -parity can be related to an element of SO(10) [33] under which a fermion field transforms into its charge conjugate. In cases where D -parity is not broken by R_1 , it is subsequently broken by R_2 at the intermediate scale M_{int} . In this work we only consider the subgroups without an explicit SU(5) factor. Since the DM is necessarily a color singlet, the running of the strong gauge coupling is unaltered by the presence of a new DM particle below the intermediate scale. Thus even though the addition of a DM multiplet yields unification of the gauge couplings, the unification scale M_{int} is always less than 10^{14} GeV as the contribution to the $\text{U}(1)_Y$ beta function is always positive. If we now associate M_{int} with SU(5), this low partial unification is heavily disfavored on the basis of proton lifetime constraints. Flipped SU(5) usually has a high intermediate scale and a high GUT scale close to the Planck scale. In this case higher dimension operators suppressed by Planck scale become important, and one may also need to rely on a double seesaw for the explanation of neutrino masses [34,35]. These bring extra complication into our model and we do not consider these possibilities here. Other intermediate gauge groups in the table are subgroups of $\text{SU}(4)_C \otimes \text{SU}(2)_L \otimes \text{SU}(2)_R \otimes D$, and $\text{U}(1)_{B-L}$ is a subgroup of $\text{SU}(4)_C$. The relationship among hypercharge Y , the $\text{U}(1)_{B-L}$ charge $B-L$, and the third component of the $\text{SU}(2)_R$ generators T_R^3 is very useful for determining the quantum numbers of DM candidates:

$$Y = \frac{B-L}{2} + T_R^3 . \quad (2)$$

The convention we are using for hypercharge is such that electric charge is given by $Q = T_L^3 + Y$, with T_L^3 denoting the third component of the $\text{SU}(2)_L$ generators.

To summarize, our model contains the usual SM content and an $\text{SU}(2)_L$ multiplet for DM at low energy scale. At the intermediate scale, depending on G_{int} there are parts of the DM SO(10) multiplet, parts of the **126** Higgs field to break G_{int} while conserving matter parity, and perhaps some other Higgs fields that we specify on a model by model

²The next-to-minimal possibility is a **1728**. In addition, we note that a \mathbb{Z}_3 symmetry can be obtained by a **672** Higgs field [23,24].

Table 1: *Candidates for the intermediate gauge group G_{int} .*

G_{int}	R_1
$SU(4)_C \otimes SU(2)_L \otimes SU(2)_R$	210
$SU(4)_C \otimes SU(2)_L \otimes SU(2)_R \otimes D$	54
$SU(4)_C \otimes SU(2)_L \otimes U(1)_R$	45
$SU(3)_C \otimes SU(2)_L \otimes SU(2)_R \otimes U(1)_{B-L}$	45
$SU(3)_C \otimes SU(2)_L \otimes SU(2)_R \otimes U(1)_{B-L} \otimes D$	210
$SU(3)_C \otimes SU(2)_L \otimes U(1)_R \otimes U(1)_{B-L}$	45, 210
$SU(5) \otimes U(1)$	45, 210
Flipped $SU(5) \otimes U(1)$	45, 210

basis and are necessary for fine-tuning the DM mass. All other components in SO(10) multiplets are assumed to be at the GUT scale.

2.2 WIMP DM candidates

In this section we discuss possible DM candidates in SO(10) representations up to **210**, and classify them according to their quantum numbers. As discussed in the last section, the stability of DM is ensured by matter parity. Thus a fermionic DM candidate should be parity even and belong to a **10**, **45**, **54**, **120**, **126**, **210** or **210'** representation, while scalar DM is parity odd and belongs to a **16** or **144** representation [8,23,24]. Following the branching rules given in Ref. [36], in Table 2, we list $SU(2)_L \otimes U(1)_Y$ multiplets in various SO(10) representations that contain an electrically neutral color singlet. A similar list of candidates can be found in earlier work [10]. The table is classified by $B - L$ so one can check the matter parity of the candidates easily; $B - L = 0, 2$ candidates are fermionic while $B - L = 1$ candidates are scalar, labeled by an “F” or “S” at the beginning of each row, respectively. The subscript of the model names denotes the $SU(2)_L$ representation, while the superscript shows hypercharge. A hat is used for $B - L = 2$ candidates.

We consider the WIMP DM scenario, which requires DM to be in thermal equilibrium with the SM particles before its abundance freezes out. This generally requires DM particles to interact with SM particles efficiently in the early universe. As a consequence, the fermionic singlets F_1^0 and \widehat{F}_1^0 are not good WIMP candidates since they are SM singlets and can only interact with SM particles through exchange of intermediate scale virtual particles. In fact, these are examples of NETDM and the possibilities for F_1^0 and \widehat{F}_1^0 candidates for DM were discussed extensively in [24]. Indeed, there it was shown that only two NETDM candidates from SO(10) survive all phenomenological constraints. One possibility is associated with the $SU(4)_C \otimes SU(2)_L \otimes SU(2)_R$ intermediate gauge group. In this case, the DM candidate is in a **(1, 1, 3)** originating in a **45**. This is an example

Table 2: List of $SU(2)_L \otimes U(1)_Y$ multiplets in $SO(10)$ representations that contain an electric neutral color singlet.

Model	$B - L$	$SU(2)_L$	Y	$SO(10)$ representations
F_1^0		1	0	45, 54, 210
$F_2^{1/2}$		2	1/2	10, 120, 126, 210'
F_3^0	0	3	0	45, 54, 210
F_3^1		3	1	54
$F_4^{1/2}$		4	1/2	210'
$F_4^{3/2}$		4	3/2	210'
S_1^0		1	0	16, 144
$S_2^{1/2}$	1	2	1/2	16, 144
S_3^0		3	0	144
S_3^1		3	1	144
\widehat{F}_1^0		1	0	126
$\widehat{F}_2^{1/2}$	2	2	1/2	210
\widehat{F}_3^1		3	1	126

of F_1^0 . The second example is based on $SU(4)_C \otimes SU(2)_L \otimes SU(2)_R \otimes D$ and consists of a $(\mathbf{15}, \mathbf{1}, \mathbf{1})$ originating from either a **45** or a **210** in $SO(10)$. Since the **15** of $SU(4)_C$ carries zero $B - L$ charge, this is also an example of F_1^0 . All possible candidates associated with \widehat{F}_1^0 were excluded in [24]. A fermion that is a singlet under the intermediate gauge group can also be produced through the exchange of the GUT scale particles, and thus be a DM candidate. For example, the case of the $(\mathbf{1}, \mathbf{1}, \mathbf{1})$ component of a **210** is discussed in Ref. [24], which is again an example of F_1^0 DM.

The scalar singlet S_1^0 and triplet S_3^0 can interact with the SM Higgs boson efficiently through the quartic coupling and are potential good DM candidates to be discussed below. These can be taken to be either real or complex. For S_1^0 , there is no difference in any of our results whether S_1^0 is real or complex. We have taken S_3^0 to be real, but there would be no qualitative difference in our results for complex S_3^0 . In addition, S_3^0 couples to the SM particles via the weak interaction. Similarly, the fermion triplet F_3^0 is a wino-like DM candidate and will also be considered below. In general, the neutral component of a $SU(2)_L \otimes U(1)_Y$ multiplet can interact with SM particles through exchange of W or Z boson, and thus can be a good DM candidate. Such DM candidates have been widely studied in the literature [37–47].

There are also DM candidates which have non-zero hypercharge. These are: $F_2^{1/2}$, F_3^1 , $F_4^{1/2}$, $F_4^{3/2}$, $S_2^{1/2}$, S_3^1 , $\widehat{F}_2^{1/2}$, and \widehat{F}_3^1 . These DM candidates are severely constrained by DM

direct detection experiments since their scattering cross sections with a nucleon induced by Z -boson exchange are generally too large. Possible ways to evade this constraint are discussed in the following section.

2.3 Hypercharged DM

A DM candidate with $Y \neq 0$ needs to be a Dirac spinor or a complex scalar, depending on its matter parity. These hypercharged candidates are severely restricted by the direct detection experiments, since they elastically scatter nucleons via the vector interactions mediated by Z -boson exchange, whose scattering cross section turns out to be too large by many orders of magnitude. One possible way to evade the constraint is to generate mass splitting, Δm , between the neutral components of such a DM multiplet ψ and to split it into two Majorana fermions or real scalars χ_1, χ_2 . Then, the DM no longer suffers from large scattering cross sections since it does not have vector interactions. Such splitting occurs if the DM mixes with extra $SU(2)_L \otimes U(1)_Y$ multiplets after electroweak symmetry breaking, just like higgsinos in the MSSM, which originally form a Dirac fermion, reduce to neutralinos after they mix with gauginos. As we have assumed that only a single DM multiplet lies in the low-energy region, a natural mass scale for the extra $SU(2)_L \otimes U(1)_Y$ multiplets is the intermediate scale M_{int} . The effects of these heavy particles on the low-energy theory are expressed in terms of effective operators induced after integrating them out. Among them, the following operator is relevant for the generation of mass splitting for Dirac fermion DM:

$$\frac{1}{M_{\text{int}}^n} \bar{\psi}^{\mathcal{C}} \psi H^{*p}, \quad (3)$$

where H is the SM Higgs field, \mathcal{C} represents charge conjugation, $p = 4Y_\psi$ with $Y_\psi > 0$ being the hypercharge of the DM ψ , and $n = p - 1$. For complex scalar DM, we have a similar operator with $n = p - 2$. Notice that the above operator violates any particle number assigned to the fermion ψ . After the Higgs field acquires a VEV, the above operator reduces to a Majorana mass term, which generates a mass splitting between two Weyl fermions inside the neutral component of the DM multiplet. Namely, the mass eigenstates are expressed by two Majorana fermions, and the lighter one can be regarded as DM. The splitting is just given by $\Delta m \sim v^p / M_{\text{int}}^n$ with $v \simeq 174$ GeV being the Higgs VEV. Since a Majorana fermion does not couple to vector interactions, DM-nucleon elastic scattering cross sections are significantly reduced and we can avoid the direct detection bound. In the case of scalars, a similar operator to that in Eq. (3) induces a splitting in the squared masses and hence $\Delta m \sim v^p / (M_{\text{int}}^n m_\psi)$ where m_ψ corresponds to the scalar mass term $m_\psi^2 \psi \psi^*$.

However, notice that the operator (3) is considerably suppressed if the intermediate scale is large [42]. The suppression becomes more significant when Y_ψ is larger. In this case, the resultant mass splitting becomes extremely small. When the mass splitting is sufficiently small, then the DM can scatter off a nucleon N inelastically: $\chi_1 + N \rightarrow \chi_2 + N$. Since this process is induced by the vector interactions, the scattering cross section again becomes too large if the mass splitting Δm is smaller than the recoil energy. This sets

the bound $\Delta m \gtrsim 100$ keV. For this condition to be satisfied, $M_{\text{int}} \lesssim 10^9$, 3×10^4 , and 4×10^3 GeV are required for fermionic dark DM with $Y_\psi = 1/2$, 1 and $3/2$, respectively [42]. In the case of scalar DM, the upper bound depends on the DM mass. For a 1 TeV DM mass, $M_{\text{int}} \lesssim 10^5$ GeV for $Y_\psi = 1$. For a $Y_\psi = 1/2$ scalar DM candidate, on the other hand, the mass splitting can be generated with a renormalizable interaction and its effect on the mass splitting depends only on its dimensionless coefficient. We will see later that this coefficient can still be very small, whose size is determined by the symmetry breaking pattern and its scale. This is because the operators relevant for the generation of the mass splitting are forbidden by the SO(10) symmetry. Thus, the constraint from inelastic scattering can again give a bound on the intermediate scale even for $Y_\psi = 1/2$ scalar DM candidates.

Another possibility to evade the direct detection bound is to push the DM mass sufficiently high. Since the local number density of DM is inversely proportional to the DM mass as the DM local energy density is fixed, the DM direct detection constraints are relaxed if the DM mass is taken to be heavy enough. In this case, DM is produced non-thermally [48]. This possibility is also discussed below.

3 Scalar dark matter

In this section, we discuss scalar WIMP DM in SO(10) models with different intermediate subgroups. In this case, the DM candidates belong to either a **16** or a **144** representation. The masses of components in a DM multiplet in general need to be fine-tuned; if a charged component is nearly degenerate with the DM particle and decays to it only through an intermediate-scale gauge boson or Higgs field, this charged particle would be very long lived, which is cosmologically disastrous [24]. Thus, to be safe, we take the masses of these extra components to be $\mathcal{O}(M_{\text{GUT}})$ or $\mathcal{O}(M_{\text{int}})$, while the DM mass to be around TeV scale so that the thermal relic abundance of the DM agrees with the observed DM density, as we will see in Sec. 3.1. Here, we assume that the fine-tuning of DM masses be realized with a minimal choice of Higgs fields, that is, we exploit only R_1 and $R_2 = \mathbf{126}$ to generate desired mass spectrum with R_1 being an irreducible representation chosen from Table 1. This is possible because a **16** or **144** can couple to the **126** Higgs field. Then, we study whether each set of matter content and its mass spectrum offers gauge coupling unification with appropriate GUT and intermediate scales. In Sec. 3.2, we present the results for the analysis and list promising candidates with M_{int} and M_{GUT} determined by means of renormalization group equations (RGEs). The fine-tuning for the masses of components in a DM multiplet is discussed in Sec. 3.3. As discussed in the previous section, hypercharged DM candidates require additional consideration for the generation of the mass splitting between the neutral components to avoid the bound from the direct detection experiments. This is discussed in Sec. 3.4. Finally, in Sec. 3.5, we summarize the current experimental constraints and future prospects for the scalar DM candidates discussed in this section.

3.1 DM mass

To determine the renormalization group (RG) running of gauge couplings, we need to know the mass of DM candidates, since they affect the running above its mass scale. An exception is \mathbf{S}_1^0 as it is a SM singlet and does not contribute to the gauge coupling beta functions below M_{int} at the one-loop level. Scalar singlet DM is discussed in Ref. [49]. To roughly estimate favored mass region for such a singlet DM particle, consider the quartic interaction between the singlet DM ϕ and the SM Higgs field: $-\lambda_{H\phi}\phi^2|H|^2/2$. Through this coupling, the singlet DM particles annihilate into a pair of the SM Higgs bosons. The annihilation cross section σ_{ann} times the relative velocity between the initial state particles v_{rel} is evaluated as

$$\sigma_{\text{ann}}v_{\text{rel}} \simeq \frac{\lambda_{H\phi}^2}{16\pi m_{\text{DM}}^2}, \quad (4)$$

assuming that the DM mass m_{DM} is much larger than the SM Higgs mass m_h and we neglect terms proportional to v^2 . The DM relic abundance is, on the other hand, related to the annihilation cross section by

$$\Omega_{\text{DM}}h^2 \simeq \frac{3 \times 10^{-27} \text{ cm}^3 \text{ s}^{-1}}{\langle \sigma_{\text{ann}}v_{\text{rel}} \rangle}. \quad (5)$$

To account for the observed DM density $\Omega_{\text{DM}}h^2 = 0.12$ [1], the DM mass should be $m_{\text{DM}} \lesssim 10$ TeV for $\lambda_{H\phi} \lesssim 1$. This gives us a rough upper bound for the DM mass.

The other scalar DM candidates are $\text{SU}(2)_L \otimes \text{U}(1)_Y$ multiplets, which can interact with SM particles through gauge interactions besides the quartic coupling mentioned above. In particular, $\mathbf{S}_2^{1/2}$ is known as the Inert Higgs Doublet Model and has been widely studied in the literature³ [50, 51]. To evaluate the effects of gauge interactions, let us first consider the limit of zero quartic couplings. In this case, the annihilation cross sections are completely determined as functions of the DM mass m_{DM} . Since the annihilation into SM fermions and Higgs boson suffers from p -wave suppression, the DM particles annihilate predominantly into the weak gauge bosons. In addition, we need to take into account coannihilation effects since all of the components in a $\text{SU}(2)_L$ multiplet are degenerate in mass; the mass difference among the components is induced after electroweak symmetry breaking at the loop level and thus is quite suppressed compared to the DM mass, as small as $\mathcal{O}(100)$ MeV. Taking these effects into account, for \mathbf{S}_n^Y , the effective (averaged) annihilation cross section is given by [37]

$$\sigma_{\text{ann}}v_{\text{rel}} \simeq \frac{g^4(3 - 4n^2 + n^4) + 16Y^4g'^4 + 8g^2g'^2Y^2(n^2 - 1)}{64\pi c_n m_{\text{DM}}^2}, \quad (6)$$

where g (g') are the $\text{SU}(2)_L$ ($\text{U}(1)_Y$) gauge couplings and $c_n = n$ ($2n$) for a real (complex) scalar. Here, we assume the DM mass to be much larger than the weak gauge boson masses. Again Eq. (5) tells us that the masses of the DM candidates should fall into a

³For another approach to the realization of the Inert Higgs doublet model based on grand unification, see Ref. [52].

region from ~ 500 GeV to ~ 2 TeV. On the other hand, if the quartic coupling is larger than the gauge couplings, the annihilation into a pair of Higgs bosons becomes dominant and thus the DM abundance would be similar to that of the singlet DM candidate. In general, the DM mass should lie between 0.5 TeV to 10 TeV for $\mathbf{S}_2^{1/2}$, \mathbf{S}_3^0 and \mathbf{S}_3^1 .

More accurate estimations for the DM mass can be found in the literature [37, 39, 53] with various additional contributions taken into account. For $SU(2)_L \otimes U(1)_Y$ DM multiplets, the non-perturbative Sommerfeld enhancement is of great importance [54]. In the limit of zero quartic coupling, the DM masses with which the relic abundance agrees with the observed DM density are evaluated as $m_{\text{DM}} = 0.5$ and 2.5 TeV for $\mathbf{S}_2^{1/2}$ and \mathbf{S}_3^0 , respectively [53]. For \mathbf{S}_3^1 , as far as we know, there has been no calculation which includes the Sommerfeld enhancement; thus its mass would be larger than 1.6 TeV, which is obtained with only the perturbative contribution considered [37]. For the cases where the scalar DM multiplets have non-zero quartic coupling with the SM Higgs doublet, it was shown in Ref. [39] that the allowed DM mass can be extended to ~ 58 and 28 TeV for $\mathbf{S}_2^{1/2}$ and \mathbf{S}_3^0 , respectively, when the quartic coupling $\lambda \sim 4\pi$. Such a large quartic coupling is, however, in general inconsistent with GUTs since it immediately blows up at a scale much below the GUT and intermediate scales. Thus, we implicitly assume the quartic coupling should be rather small, *e.g.*, $\lesssim 1$, to avoid divergent couplings. In this case, the DM mass usually lies around $\mathcal{O}(1)$ TeV.

3.2 Candidates for scalar DM

We list all possible scalar DM candidates in Table 3. All of the candidates belong to either a **16** or a **144**. Here, the first column shows the model names with subscript representing the intermediate gauge group G_{int} . The second column lists the G_{int} representations that contain the DM candidate multiplet \mathbf{S}_n^Y . All of the components in the representation except the DM multiplet \mathbf{S}_n^Y shown in the third column will have masses tuned to $\mathcal{O}(M_{\text{int}})$. The rest of the components in the $SO(10)$ multiplet have masses of $\mathcal{O}(M_{\text{GUT}})$. The case of $G_{\text{int}} = SU(4)_C \otimes SU(2)_L \otimes SU(2)_R \otimes D$ ($SU(3)_C \otimes SU(2)_L \otimes SU(2)_R \otimes U(1)_{B-L} \otimes D$) is identical to that of $G_{\text{int}} = SU(4)_C \otimes SU(2)_L \otimes SU(2)_R$ ($SU(3)_C \otimes SU(2)_L \otimes SU(2)_R \otimes U(1)_{B-L}$) with additional multiplets required by the left-right symmetry introduced above the intermediate scale.

Consider, for example, \mathbf{SA}_{422} ; the $(\mathbf{4}, \mathbf{1}, \mathbf{2})$ DM multiplet originating from a **16** of $SO(10)$ in the $SU(4)_C \otimes SU(2)_L \otimes SU(2)_R$ model. The ‘‘other half’’ of the **16**, $(\mathbf{4}, \mathbf{2}, \mathbf{1})$, will have a GUT scale mass, while 7 of 8 fields in $(\mathbf{4}, \mathbf{1}, \mathbf{2})$ are tuned to have an intermediate scale mass and only the DM singlet is tuned to have a weak scale mass. In the case of \mathbf{SA}_{422D} , the DM multiplet corresponds to the $(\mathbf{4}, \mathbf{1}, \mathbf{2}) \oplus (\bar{\mathbf{4}}, \mathbf{2}, \mathbf{1})$ in the $SU(4)_C \otimes SU(2)_L \otimes SU(2)_R \otimes D$ model. In this case, none of the components have GUT scale masses and 15 of the 16 fields have intermediate scale masses. Thus the presence of the left-right symmetry affects only the field content above the intermediate scale, though this will ultimately affect the scale of gauge coupling unification. These representations are added to a minimal $SO(10)$ unification model containing three generations of **16** chiral multiplet, a complex **10** Higgs multiplet, a $R_2 = \mathbf{126}$ Higgs multiplet, and a R_1 Higgs multiplet

Table 3: Summary of DM multiplets. The second column shows the G_{int} representation with quantum numbers listed in the same order as the groups shown in the direct product. The case of $G_{\text{int}} = SU(4)_C \otimes SU(2)_L \otimes SU(2)_R \otimes D$ ($SU(3)_C \otimes SU(2)_L \otimes SU(2)_R \otimes U(1)_{B-L} \otimes D$) is identical to that of $G_{\text{int}} = SU(4)_C \otimes SU(2)_L \otimes SU(2)_R$ ($SU(3)_C \otimes SU(2)_L \otimes SU(2)_R \otimes U(1)_{B-L}$) with additional multiplets required by left-right symmetry introduced above the intermediate scale.

Model	R_{DM}	S_n^Y	SO(10) representation
$G_{\text{int}} = SU(4)_C \otimes SU(2)_L \otimes SU(2)_R (\otimes D)$			
SA _{422(D)}	4, 1, 2	S_1^0	16, 144
SB _{422(D)}	4, 2, 1	$S_2^{1/2}$	16, 144
SC _{422(D)}	4, 2, 3	$S_2^{1/2}$	144
SD _{422(D)}	4, 3, 2	S_3^1	144
SE _{422(D)}	4, 3, 2	S_3^0	144
$G_{\text{int}} = SU(4)_C \otimes SU(2)_L \otimes U(1)_R$			
SA ₄₂₁	4, 1, -1/2	S_1^0	16, 144
SB ₄₂₁	4, 2, 0	$S_2^{1/2}$	16, 144
SC ₄₂₁	4, 2, 1	$S_2^{1/2}$	144
SD ₄₂₁	4, 3, 1/2	S_3^1	144
SE ₄₂₁	4, 3, -1/2	S_3^0	144
$G_{\text{int}} = SU(3)_C \otimes SU(2)_L \otimes SU(2)_R \otimes U(1)_{B-L} (\otimes D)$			
SA _{3221(D)}	1, 1, 2, 1	S_1^0	16, 144
SB _{3221(D)}	1, 2, 1, -1	$S_2^{1/2}$	16, 144
SC _{3221(D)}	1, 2, 3, -1	$S_2^{1/2}$	144
SD _{3221(D)}	1, 3, 2, 1	S_3^1	144
SE _{3221(D)}	1, 3, 2, 1	S_3^0	144

chosen from Table 1. Notice that $S_2^{1/2}$ is contained in both the model SB's and SC's. The difference between the models is the $SU(2)_R$ (or additional $U(1)$) charge assignment; for instance, SB₄₂₂ (SC₄₂₂) includes the $SU(2)_R$ singlet (triplet) DM. From Table 3, we find that a **16** contains only SA's and SB's, while a **144** has all of the candidates listed in the table.

Next, we perform the RGE⁴ analysis in the models presented in Table 3 to see if these models achieve gauge coupling unification with appropriate GUT and intermediate scales. The one-loop results for M_{GUT} , M_{int} , the unified gauge coupling α_{GUT} , and the proton

⁴The beta functions for the minimal SO(10) GUT described above are given in Appendix B of Ref. [24].

Table 4: *One-loop result for scales, unified couplings, and proton lifetimes for models in table. 3. The DM mass is set to be $m_{DM} = 1$ TeV. The mass scales are given in GeV and the proton lifetimes are in units of years. Blue shaded models evade the proton decay bound, $\tau(p \rightarrow e^+\pi^0) > 1.4 \times 10^{34}$ yrs [55, 56].*

Model	$\log_{10} M_{\text{GUT}}$	$\log_{10} M_{\text{int}}$	α_{GUT}	$\log_{10} \tau_p(p \rightarrow e^+\pi^0)$
$G_{\text{int}} = \text{SU}(4)_C \otimes \text{SU}(2)_L \otimes \text{SU}(2)_R$				
SA ₄₂₂	16.33	11.08	0.0218	36.8 ± 1.2
SB ₄₂₂	15.62	12.38	0.0228	34.0 ± 1.2
SC ₄₂₂	14.89	11.18	0.0243	31.0 ± 1.2
SD ₄₂₂	14.11	13.29	0.0253	28.0 ± 1.2
SE ₄₂₂	14.73	13.72	0.0243	30.4 ± 1.2
$G_{\text{int}} = \text{SU}(4)_C \otimes \text{SU}(2)_L \otimes \text{SU}(2)_R \otimes D$				
SA _{422D}	15.23	13.71	0.0245	32.4 ± 1.2
SB _{422D}	15.01	13.71	0.0247	31.6 ± 1.2
SC _{422D}	14.50	13.71	0.0254	29.5 ± 1.2
SD _{422D}	13.95	13.47	0.0260	27.3 ± 1.2
SE _{422D}	14.55	13.96	0.0251	29.7 ± 1.2
$G_{\text{int}} = \text{SU}(4)_C \otimes \text{SU}(2)_L \otimes \text{U}(1)_R$				
SA ₄₂₁	14.62	10.96	0.0226	30.1 ± 1.2
SB ₄₂₁	14.55	11.90	0.0233	29.8 ± 1.2
SC ₄₂₁	14.15	10.92	0.0236	28.2 ± 1.2
SD ₄₂₁	13.91	12.80	0.0250	27.2 ± 1.2
SE ₄₂₁	14.45	13.12	0.0241	29.4 ± 1.2
$G_{\text{int}} = \text{SU}(3)_C \otimes \text{SU}(2)_L \otimes \text{SU}(2)_R \otimes \text{U}(1)_{B-L}$				
SA ₃₂₂₁	16.66	8.54	0.0217	38.1 ± 1.2
SB ₃₂₂₁	16.17	9.80	0.0223	36.2 ± 1.2
SC ₃₂₂₁	15.62	9.14	0.0230	34.0 ± 1.2
SD ₃₂₂₁	14.49	12.07	0.0246	29.5 ± 1.2
SE ₃₂₂₁	15.09	12.22	0.0237	31.9 ± 1.2
$G_{\text{int}} = \text{SU}(3)_C \otimes \text{SU}(2)_L \otimes \text{SU}(2)_R \otimes \text{U}(1)_{B-L} \otimes D$				
SA _{3221D}	15.58	10.08	0.0231	33.8 ± 1.2
SB _{3221D}	15.40	10.44	0.0233	33.1 ± 1.2
SC _{3221D}	14.58	11.62	0.0245	29.8 ± 1.2
SD _{3221D}	14.07	12.13	0.0253	27.8 ± 1.2
SE _{3221D}	14.60	12.29	0.0245	29.9 ± 1.2

lifetimes in the $p \rightarrow e^+\pi^0$ channel are shown in Table 4.⁵ Here, M_{GUT} and M_{int} are given in GeV units, while the unit for proton lifetimes $\tau_p(p \rightarrow e^+\pi^0)$ is years. The DM mass is set to be $m_{\text{DM}} = 1$ TeV. We have checked that altering the DM mass by an order of magnitude results in only a $\mathcal{O}(0.2)\%$ variation in the logarithmic masses of M_{int} and M_{GUT} . The uncertainty of the lifetime reflects our innocence of the GUT-scale gauge boson mass M_X , which we take it to be within a range of $0.5M_{\text{GUT}} \lesssim M_X \lesssim 2M_{\text{GUT}}$. It turns out that most models have already been ruled out by the current experimental constraint $\tau(p \rightarrow e^+\pi^0) > 1.4 \times 10^{34}$ yrs [55, 56]. The models that possibly survive this constraint are **SA**₄₂₂, **SB**₄₂₂, **SA**₃₂₂₁, **SB**₃₂₂₁, **SC**₃₂₂₁, **SA**_{3221D}, and **SB**_{3221D}, which are highlighted in blue shading in the table. In terms of $\text{SU}(2)_L \otimes \text{U}(1)_Y$ assignments, only **S**₁⁰ and **S**₂^{1/2} are found to be viable candidates. Among them, models **SB**₄₂₂, **SC**₃₂₂₁, **SA**_{3221D}, and **SB**_{3221D} predict proton lifetimes close to the present limit, and thus can be tested in future proton decay experiments.

3.3 Fine-tuning of scalar DM multiplets

In the previous section, we have reduced the possibilities for G_{int} to the only three gauge groups: $\text{SU}(4)_C \otimes \text{SU}(2)_L \otimes \text{SU}(2)_R$, $\text{SU}(3)_C \otimes \text{SU}(2)_L \otimes \text{SU}(2)_R \otimes \text{U}(1)_{B-L}$, and $\text{SU}(3)_C \otimes \text{SU}(2)_L \otimes \text{SU}(2)_R \otimes \text{U}(1)_{B-L} \otimes D$. According to Table 1, $R_1 = \mathbf{210}$, $\mathbf{45}$, and $\mathbf{210}$ yield the above intermediate gauge groups, respectively. In this section, we briefly discuss how to obtain a desired mass spectrum for the DM multiplet using these R_1 's and $R_2 = \mathbf{126}$ with the help of fine-tuning. For convenience, we show an explicit procedure for the fine-tuning in Appendix C, by taking $R_{\text{DM}} = \mathbf{16}$ and $G_{\text{int}} = \text{SU}(3)_C \otimes \text{SU}(2)_L \otimes \text{SU}(2)_R \otimes \text{U}(1)_{B-L}$ as an example.

Let us first write down relevant terms for the mass terms of the DM multiplet R_{DM} .⁶

$$\begin{aligned}
-\mathcal{L}_{\text{int}} = & M^2 |R_{\text{DM}}|^2 + \kappa_1 R_{\text{DM}}^* R_{\text{DM}} R_1 + \{\kappa_2 R_{\text{DM}} R_{\text{DM}} R_2^* + \text{h.c.}\} \\
& + \lambda_1^1 |R_{\text{DM}}|^2 |R_1|^2 + \lambda_2^1 |R_{\text{DM}}|^2 |R_2|^2 + \{\lambda_{12}^{\mathbf{126}} (R_{\text{DM}} R_{\text{DM}})_{\mathbf{126}} (R_1 R_2^*)_{\overline{\mathbf{126}}} + \text{h.c.}\} \\
& + \lambda_1^{\mathbf{45}} (R_{\text{DM}}^* R_{\text{DM}})_{\mathbf{45}} (R_1^* R_1)_{\mathbf{45}} + \lambda_1^{\mathbf{210}} (R_{\text{DM}}^* R_{\text{DM}})_{\mathbf{210}} (R_1^* R_1)_{\mathbf{210}} \\
& + \lambda_2^{\mathbf{45}} (R_{\text{DM}}^* R_{\text{DM}})_{\mathbf{45}} (R_2^* R_2)_{\mathbf{45}} + \lambda_2^{\mathbf{210}} (R_{\text{DM}}^* R_{\text{DM}})_{\mathbf{210}} (R_2^* R_2)_{\mathbf{210}} , \tag{7}
\end{aligned}$$

where the subscripts after the parentheses denote the $\text{SO}(10)$ representation formed by the product in them. M , κ_1 , and κ_2 are dimensionful parameters, which we assume to be $\mathcal{O}(M_{\text{GUT}})$. Notice that the term $(R_{\text{DM}} R_{\text{DM}})_{\mathbf{120}} (R_1 R_2^*)_{\mathbf{120}}$ and its charge conjugate vanish since the R_{DM} is a bosonic field and $(AB)_{\mathbf{120}}$ is anti-symmetric with respect to the exchange of A and B . In addition, the term $(R_{\text{DM}} R_{\text{DM}})_{\mathbf{10}} (R_1 R_2^*)_{\mathbf{10}}$ does not give a mass term for R_{DM} ; $\langle R_1 R_2^* \rangle$ is singlet with respect to the SM gauge interactions, and a $\mathbf{10}$ representation does not contain such a component. The terms with the coefficients

⁵We restrict our attention to one-loop running as two loop effects become very model dependent on our choice of the scalar potential.

⁶In addition, there are couplings between the DM and the SM Higgs fields, which give a mass of the order of the electroweak scale to the DM multiplet.

λ_1^1 and λ_2^1 are irrelevant to the generation of the mass splitting in the DM multiplet, as they only give a common mass to all of the components in the multiplet. It is also worth noting that terms including κ_2 and λ_{12}^{126} break the particle number which can be assigned to the complex scalar R_{DM} . Hence, these effects can split R_{DM} into two real scalars with different masses. We use these interactions to avoid the direct detection bound in the case of the complex hypercharged DM, models SB's and SC's, which we discuss in the following section.

After R_1 gets a VEV, the terms with κ_1 , λ_1^{45} , and λ_1^{210} generate mass terms for the components in R_{DM} with different mass values, since the R_1 VEV couples to them with different Clebsch-Gordan coefficients. Thus, by fine tuning the coefficients M , κ_1 , λ_1^{45} , and λ_1^{210} , one can arrange that the DM multiplet obtains a mass of $\mathcal{O}(M_{\text{int}})$, with other multiplets remaining around $\mathcal{O}(M_{\text{GUT}})$.

The next step is to separate the $\text{SU}(2)_L$ multiplet \mathbf{S}_n^Y from the intermediate gauge group multiplet. This can be accomplished by appropriately tuning the coefficients of κ_2 , λ_{12}^{126} , λ_2^{45} , and λ_2^{210} so that the generated mass terms cancel out the intermediate scale mass obtained previously, leaving only the DM candidate at TeV scale.⁷ After this step, we obtain a mass spectrum in which only the DM candidate lies around the TeV scale, while its partner fields with respect to the intermediate gauge symmetry are at M_{int} . The rest of the components of R_{DM} have masses of $\mathcal{O}(M_{\text{GUT}})$. For an explicit example, see Appendix B.

3.4 Mass splitting of hypercharged scalar dark matter

As discussed in Sec. 2.3, we need a mass splitting of $\Delta m \gtrsim 100\text{keV}$ [42] between the neutral and charged components of the hypercharged DM candidates (models SB and SC) to avoid the direct detection bound. Since both of these models yield $\mathbf{S}_2^{1/2}$ DM, the mass splitting can be induced by dimension-four operators like $\phi^2 H^{*2}$, where ϕ denotes the hypercharged scalar DM $\mathbf{S}_2^{1/2}$. Such operators are, however, forbidden by the $\text{SO}(10)$ GUT symmetry; in fact, as the $\mathbf{S}_2^{1/2}$ DM and the SM Higgs field have $B - L = 1$ and 0, respectively, the operators contributing the mass splitting violate the $B - L$ symmetry. Thus, they can be induced only below the intermediate scale where the $B - L$ symmetry is spontaneously broken.

Such an operator is induced by the interactions with the coefficients κ_2 and λ_{12}^{126} in Eq. (7), since it requires violation of the particle number associated with the DM field ϕ . The required $B - L$ breaking is realized by the R_2 VEV. We find that the tree-level diagrams in Fig. 1 are relevant to the generation of mass splitting. Here, $R_H = \mathbf{10}$

⁷In the cases of models SB and SC, however, terms with κ_2 and λ_{12}^{126} do not give mass terms for the DM multiplet after the intermediate symmetry breaking. The reason is as follows. For SB, since the R_2 VEV has a $\text{SU}(2)_R$ charge while SB DM candidates do not, the couplings between the R_2 VEV and the SB DM are forbidden by the $\text{SU}(2)_R$ symmetry. For SC's, since both the DM candidates and the R_2 VEV are in $\text{SU}(2)_R$ triplets, a pair of the DM fields should be combined anti-symmetrically to be coupled to the R_2 VEV, but this vanishes because the DM is bosonic. In these cases, therefore, we carry out the fine-tuning for the DM mass only with the coefficients λ_2^{45} and λ_2^{210} .

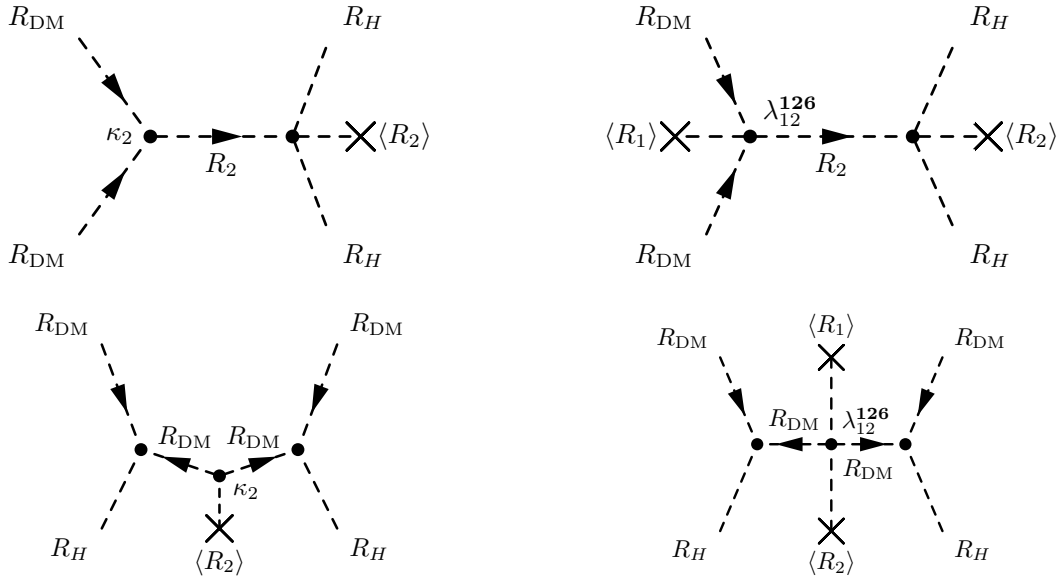


Figure 1: *Diagrams that generate the mass splitting between real components of hypercharged scalar DM.*

contains the SM Higgs field. Since the κ_2 and λ_{12}^{126} interactions are symmetric with respect to the interchange of R_{DM} , the component in R_2 which propagates in the upper two diagrams should be an $\text{SU}(2)_L$ triplet. On the other hand, the component appearing in the inner lines in the lower two diagrams can be either an $\text{SU}(2)_L$ singlet or triplet. The masses of these fields are dependent on the intermediate gauge groups; if $G_{\text{int}} = \text{SU}(4)_C \otimes \text{SU}(2)_L \otimes \text{SU}(2)_R$ or $\text{SU}(3)_C \otimes \text{SU}(2)_L \otimes \text{SU}(2)_R \otimes \text{U}(1)_{B-L}$, then these masses are $\mathcal{O}(M_{\text{GUT}})$, while for $G_{\text{int}} = \text{SU}(3)_C \otimes \text{SU}(2)_L \otimes \text{SU}(2)_R \otimes \text{U}(1)_{B-L} \otimes D$, they are $\mathcal{O}(M_{\text{int}})$ because of the left-right parity D .

Let us first consider the former cases. In these cases, the coefficient of the dimension-four operator $\phi^2 H^{*2}$ is $\mathcal{O}(M_{\text{int}}/M_{\text{GUT}})$, as the dimensionful couplings in the Lagrangian are expected to be $\mathcal{O}(M_{\text{GUT}})$. We note here that there is no requirement for the cancellation between κ_2 and $\lambda_{12}^{126}\langle R_1 \rangle$ to realize the desired mass spectrum since these couplings do not contribute to the mass splitting as mentioned in footnote 7, in contrast to the case we discuss below. Thus, this operator induces a mass splitting of

$$\Delta m \sim \frac{M_{\text{int}} v^2}{m_{\text{DM}} M_{\text{GUT}}} . \quad (8)$$

The condition $\Delta m \gtrsim 100$ keV then becomes

$$\frac{M_{\text{int}}}{M_{\text{GUT}}} \gtrsim 3 \times 10^{-6} \times \left(\frac{m_{\text{DM}}}{1 \text{ TeV}} \right) . \quad (9)$$

From Table 4, we find that the model SB_{422} clearly satisfies this bound, while the intermediate scales in SB_{3221} and SC_{3221} lie slightly below this constraint. However, since this

bound is just a rough estimation and the intermediate scales given in Table 4 are obtained with the one-loop RGEs, it is possible that the DM candidates in these models are just not yet reached by the current direct detection experiments. If so, these models can be probed in the near future.

For $\text{SB}_{3221\text{D}}$, on the other hand, the mass spectrum is altered because of the presence of the left-right parity. In this case, the charge of the DM candidate under G_{int} is $(\mathbf{1}, \mathbf{2}, \mathbf{1}, -1)$, and the left-right symmetry requires the $(\mathbf{1}, \mathbf{1}, \mathbf{2}, +1)$ to be also light. To that end, the fine-tuning between the κ_2 and $\lambda_{12}^{\mathbf{126}}$ terms in Eq. 7 is required such that $\kappa_2 + \lambda_{12}^{\mathbf{126}}\langle R_1 \rangle \simeq M_{\text{int}}$; otherwise, these terms give a mass of $\mathcal{O}(\sqrt{M_{\text{int}}M_{\text{GUT}}})$ to the $(\mathbf{1}, \mathbf{1}, \mathbf{2}, +1)$ component, which is much higher than the intermediate scale. This fine-tuning also guarantees the absence of non-perturbative couplings at low energies; without this fine-tuning, the exchange of intermediate-scale particles with the κ_2 and $\lambda_{12}^{\mathbf{126}}\langle R_1 \rangle$ vertices induces extremely large effective couplings, which destroy the perturbativity of the low-energy theory.

In the presence of the fine-tuning, the diagrams in Fig. 1 with the virtual states having a mass of M_{int} induce the effective operator $\phi^2 H^{*2}$ with a coefficient of $\mathcal{O}(1)$. Thus, the resultant mass splitting is well above 100 keV and the model $\text{SB}_{3221\text{D}}$ easily evades the constraints from the direct detection experiments.

To summarize, SB_{422} and $\text{SB}_{3221\text{D}}$ are safe from the direct detection bound. SB_{3221} and SC_{3221} lie just around the margin of the bound, and they might be detected or completely excluded in future direct detection experiments.

3.5 Constraints and prospects for the scalar DM candidates

The above discussions have revealed that the only possible scalar DM candidates we could obtain with sufficiently high M_{GUT} are \mathbf{S}_1^0 and $\mathbf{S}_2^{1/2}$, as shown in Table 4. Before concluding this section, we briefly review the current constraints on these DM candidates, and give prospects for probing them in future experiments.

First, we consider \mathbf{S}_1^0 . This DM candidate has been widely discussed so far since it is one of the simplest extensions of the SM to include a DM candidate [49]. As we have seen in Sec. 3.1, the thermal relic abundance of \mathbf{S}_1^0 is determined once we fix the DM mass m_{DM} and its quartic coupling to the SM Higgs field, $\lambda_{H\phi}$. Therefore, by requiring its thermal relic abundance to be equal to the observed DM density $\Omega_{\text{DM}}h^2 = 0.12$, we can express $\lambda_{H\phi}$ as a function of the DM mass m_{DM} . Since this is the only coupling that connects the DM to the SM sector, various physical quantities relevant to the DM detection, such as the DM-nucleon scattering cross section, are also determined in terms of the DM mass.

The present constraints on this DM are summarized in Refs. [57, 58]. According to those results, currently, DM direct detection experiments give a stringent limit on the DM mass; the \mathbf{S}_1^0 DM with a mass of $m_{\text{DM}} \lesssim 53$ GeV and 64 GeV $\lesssim m_{\text{DM}} \lesssim 100$ GeV has been excluded by the LUX experiment [59]. In addition, if $m_{\text{DM}} < m_h/2$ with $m_h \simeq 125$ GeV the Higgs mass, then the constraint on the invisible decay width of the Higgs boson also restricts the DM. It turns out that the current upper bound on the invisible decay width $\text{BR}(h \rightarrow \text{invisible}) < 0.19$ [60] leads to the limit on the DM mass of $m_{\text{DM}} \gtrsim 53$ GeV. The

DM direct detection experiments with ton-scale detectors, such as XENON1T, will probe most of the DM mass region, and thus this DM model can be tested in the near future.

DM described by model $\mathbf{S}_2^{1/2}$ is called the Inert Higgs Doublet DM [50], whose current status is summarized in Refs. [51, 58]. As discussed in these papers, favored mass regions for the $\mathbf{S}_2^{1/2}$ DM that account for the correct DM abundance can be divided into two parts: $m_{\text{DM}} \lesssim 100$ GeV and $m_{\text{DM}} \gtrsim 500$ GeV. In the former case, the DM particles annihilate efficiently through the Higgs boson exchange process, especially where $m_{\text{DM}} \simeq m_h/2$. When $100 \text{ GeV} \lesssim m_{\text{DM}} \lesssim 500 \text{ GeV}$, the DM annihilation cross section is too large because the W^+W^- channel is open. For $m_{\text{DM}} \gtrsim 500 \text{ GeV}$, both the Higgs boson and the gauge bosons contribute to the DM annihilation so that the resultant relic abundance can agree to the observed DM density. For the lower mass region, the direct detection experiments, the measurements of the Higgs decay branching ratios, and the electroweak precision measurements restrict the parameter space. Both of the mass regions can be probed in future direct detection experiments [61]. Indirect detection experiments are, on the other hand, less promising; still, depending on the DM profile, gamma-ray searches from the Galactic Center may provide a signature of this DM candidate.

4 Fermionic dark matter

Next, we consider the fermionic DM candidates. Again, we begin with showing the favored mass region for these DM candidates in Sec. 4.1. As already mentioned above, the singlet fermion candidates, \mathbf{F}_1^0 and $\widehat{\mathbf{F}}_1^0$, are not good candidates for WIMP DM since their annihilation cross sections are extremely suppressed (though they are good NETDM candidates). On the other hand, electroweakly charged DM can yield the desired relic abundance via gauge interactions. We discuss the $Y = 0$ and $Y \neq 0$ cases in Sec. 4.2 and Sec. 4.3, respectively. We give some concrete examples for each case and perform RGE analysis to determine the intermediate/GUT scales of the models. Finally, in Sec. 4.4, we summarize the present limits on these fermion DM models and discuss future prospects for probing these DM candidates. Non-thermal hypercharged DM is discussed in Sec. 4.5.

4.1 DM mass

Contrary to the case of the scalar DM, the thermal relic abundance of the fermionic DM candidates is completely determined by gauge interactions. Therefore, it is possible to make a robust prediction for the DM mass favored by the present DM density. In the case of fermion DM, not only the gauge boson channels but also the SM fermions and the Higgs boson final states can contribute to s -wave annihilation. We obtain a similar expression to Eq. (6) for the effective annihilation cross section of \mathbf{F}_n^Y as [37]

$$\sigma_{\text{ann}} v_{\text{rel}} \simeq \frac{g^4(2n^4 + 17n^2 - 19) + 4Y^2 g'^4(41 + 8Y^2) + 16g^2 g'^2 Y^2 (n^2 - 1)}{128\pi c_n m_{\text{DM}}^2}, \quad (10)$$

with $c_n = 2n$ ($4n$) for a Majorana (Dirac) fermion. In addition, the Sommerfeld enhancement again affects the annihilation cross section significantly. With this effect taken

into account, the thermal relic abundance of \mathbf{F}_3^0 is computed in Ref. [62] and found to be consistent with the observed DM density if $m_{\text{DM}} \simeq 2.7$ TeV as in the case of supersymmetric winos. As for $\mathbf{F}_2^{1/2}$ and $\widehat{\mathbf{F}}_2^{1/2}$, the favored mass value is $\simeq 1.1$ TeV [37] as in the case of supersymmetric Higgsinos. As far as we know, there is no calculation for the other fermionic DM candidates that includes the Sommerfeld enhancement; without the effect, the thermal relic of \mathbf{F}_3^1 , $\widehat{\mathbf{F}}_3^1$, $\mathbf{F}_4^{1/2}$, and $\mathbf{F}_4^{3/2}$ is consistent with the observed value if $m_{\text{DM}} \simeq 1.9$ TeV, 1.9 TeV, 2.4 TeV, and 2.6 TeV, respectively [53].

4.2 Real triplet DM

We begin our discussion of fermionic DM models with the $Y = 0$ case. As discussed earlier, these are less constrained by direct detection experiments. According to Table 2, such candidates belong to $\text{SU}(2)_L$ triplets in a **45**, **54** or **210** of $\text{SO}(10)$. A summary of $\text{SU}(4)_C \otimes \text{SU}(2)_L \otimes \text{SU}(2)_R$ quantum numbers of these DM multiplets are listed in Table. 5. Note that the $B-L$ and T_R^3 charges for all of these DM candidates vanish, and therefore they are regarded as real Majorana fermions. As in the scalar DM scenario, the DM multiplet in the **54** or **210** is degenerate with other components with respect to G_{int} , and we are required to break this degeneracy to avoid unwanted long-lived colored/charged particles [24]. In the fermionic case, however, a renormalizable Yukawa term like $\overline{R}_{\text{DM}} R_{\text{DM}} \mathbf{126}_H$ is forbidden by $\text{SO}(10)$ symmetry and the choice of DM representation [24], and thus we are unable to use the **126** Higgs to break the degeneracy. Therefore, we need to introduce additional Higgs fields at the intermediate scale in these cases.

Table 5: *Real triplet DM candidates in various $\text{SO}(10)$ representations.*

$\text{SO}(10)$ representation	$\text{SU}(4)_C \otimes \text{SU}(2)_L \otimes \text{SU}(2)_R$
45	(1, 3, 1)
54	(1, 3, 3)
210	(15, 3, 1)

For simplicity, we restrict ourselves to the cases where the intermediate scale VEVs develop in the SM singlet direction of R_1 and/or $R_2 = \mathbf{126}$. One of the SM singlet components of R_1 should have a VEV of $\mathcal{O}(M_{\text{GUT}})$ to break $\text{SO}(10)$ into G_{int} . The R_2 Higgs field acquires an $\mathcal{O}(M_{\text{int}})$ VEV to break G_{int} , but it is not able to give mass differences among the components in R_{DM} , as mentioned above. Thus, we need to exploit an extra SM singlet component in R_1 which remains light compared to the GUT scale, to induce intermediate-scale mass terms for R_{DM} , which are to be used to generate the required mass splitting. We denote the VEVs of these two components of R_1 which break $\text{SO}(10)$ and G_{int} by $v_{\text{GUT}} \sim M_{\text{GUT}}$ and $v_{\text{int}} \sim M_{\text{int}}$, respectively. Then, the mass splitting

in the DM multiplet R_{DM} can be realized as follows:

$$\begin{aligned}
-\mathcal{L}_{\text{DM}} &= M\bar{R}_{\text{DM}}R_{\text{DM}} - R_1\bar{R}_{\text{DM}}R_{\text{DM}} \\
&\rightarrow (M - c_1v_{\text{GUT}} - c_2v_{\text{int}})\bar{\chi}\chi,
\end{aligned}
\tag{11}$$

where χ denotes the DM field and $M \sim M_{\text{GUT}}$ is a universal mass. c_1 and c_2 are the Clebsch-Gordan coefficients that vary for different R_{DM} components. Thus, by fine-tuning M such that $M - c_1v_{\text{GUT}} - c_2v_{\text{int}} \sim 1$ TeV, we can set the DM triplet to be at TeV scale while leaving other contents in R_{DM} either around M_{int} or M_{GUT} . We summarize in Table 6 the multiplets in R_1 that may develop a VEV of $\mathcal{O}(M_{\text{int}})$ for different G_{int} . The multiplets are labeled by the quantum numbers of G_{int} . It turns out that there is no extra SM singlet component in **54**, which is indicated by a hyphen in the table. As a consequence, there is no way to fine-tune the mass of the $(\mathbf{1}, \mathbf{3}, \mathbf{3})$ DM candidate originating from the **54** and we drop it from further discussion. Here, we note that the cases of $G_{\text{int}} = \text{SU}(3)_C \otimes \text{SU}(2)_L \otimes \text{SU}(2)_R \otimes \text{U}(1)_{B-L}$ and $\text{SU}(3)_C \otimes \text{SU}(2)_L \otimes \text{SU}(2)_R \otimes \text{U}(1)_{B-L} \otimes D$ are disfavored before further analysis: the addition of a real triplet DM lowers the unification scale to unacceptable values and in these cases there is neither any new-physics contribution to the $\text{SU}(3)_C$ gauge coupling beta function nor any new positive contribution to the $\text{SU}(2)_L$ beta function above M_{int} . Therefore, the resultant M_{GUT} is always smaller than the unification scale of the $\text{SU}(3)_C$ and $\text{SU}(2)_L$ gauge couplings in the SM plus a real triplet DM, which is below 10^{15} GeV and thus too low to evade the proton decay constraint.⁸ For this reason, we do not consider these cases in Table 6.

Table 6: *Possible components in R_1 that can develop a VEV of $\mathcal{O}(M_{\text{int}})$.*

G_{int}	R_1	Intermediate scale multiplets
$\text{SU}(4)_C \otimes \text{SU}(2)_L \otimes \text{SU}(2)_R$	210	$(\mathbf{15}, \mathbf{1}, \mathbf{1})$ $(\mathbf{15}, \mathbf{1}, \mathbf{3})$
$\text{SU}(4)_C \otimes \text{SU}(2)_L \otimes \text{SU}(2)_R \otimes D$	54	–
$\text{SU}(4)_C \otimes \text{SU}(2)_L \otimes \text{U}(1)_R$	45	$(\mathbf{15}, \mathbf{1}, 0)$

We now perform the RG analysis to look for promising models with additional intermediate Higgs multiplets given in Table 6. The one-loop results for M_{GUT} , M_{int} , α_{GUT} , and proton lifetimes for different combination of R_{DM} and the Higgs fields are listed in Table 7.⁹ Here, we set the DM mass to be 1 TeV. The second column lists the extra Higgs fields in R_1 at M_{int} in addition to R_2 . We suppressed combinations of Higgs multiplets

⁸Note that scalar doublet DM is allowed under these intermediate symmetries as shown in Table 4, since its contribution to the beta functions is much smaller than that from a fermionic real triplet, thus allowing for a higher unification scale.

⁹We again restrict our attention to one-loop RGEs to avoid any model dependence due to the Yukawa coupling with the additional Higgs in R_1 .

Table 7: *The one-loop results for M_{GUT} , M_{int} , α_{GUT} , and proton lifetimes for real triplet fermionic DM models. Here we set the DM mass to be 1 TeV. The mass scales and proton decay lifetime are in unit of GeV and years, respectively. In the blue shaded model, gauge coupling unification is achieved with a sufficiently high GUT scale.*

R_{DM}	Additional Higgs in R_1	$\log_{10} M_{int}$	$\log_{10} M_{GUT}$	α_{GUT}	$\log_{10} \tau_p(p \rightarrow e^+ \pi^0)$
$G_{int} = SU(4)_C \otimes SU(2)_L \otimes SU(2)_R$					
(1, 3, 1)	–	15.50	13.69	0.0263	–
(1, 3, 1)	(15, 1, 3)	–	–	–	–
(1, 3, 1)	(15, 1, 1)	15.65	13.47	0.0263	–
(1, 3, 1)	(15, 1, 1) (15, 1, 3)	6.54	17.17	0.0252	39.8 ± 1.2
(15, 3, 1)	(15, 1, 1)	14.44	14.10	0.0246	–
(15, 3, 1)	(15, 1, 1) (15, 1, 3)	14.52	14.11	0.0243	–
$G_{int} = SU(4)_C \otimes SU(2)_L \otimes SU(2)_R \otimes D$					
(1, 3, 1)	–	14.78	14.04	0.0250	–
$G_{int} = SU(4)_C \otimes SU(2)_L \otimes U(1)_R$					
(15, 3, 0)	(15, 1, 0)	14.55	14.21	0.0246	–

that cannot split the degeneracy of DM multiplet as in Eq. (11). The mass scales and proton decay lifetime are in units of GeV and years, respectively. We find that there is only one promising model with $G_{int} = SU(4)_C \otimes SU(2)_L \otimes SU(2)_R$, which is highlighted by blue shading in Table. 7. In this case, since the DM multiplet is a singlet under both $SU(4)_C$ and $SU(2)_R$, the additional Higgs fields are not necessary from the viewpoint of the mass splitting for the DM multiplet; namely, there is no degeneracy problem for this model. Rather, they are required so that the model achieves a good unification scale beyond proton decay constraint. The model has, however, a quite low intermediate scale that results in large neutrino masses through the type-I seesaw mechanism since the Dirac mass terms for neutrinos are related to the up-type Yukawa couplings in this setup. A simple way to evade this problem is to introduce a complex $(\mathbf{15}, \mathbf{2}, \mathbf{2})_C$ Higgs field in a $\mathbf{126}$ to modify the relation, as discussed in Ref. [24].¹⁰ If a $(\mathbf{15}, \mathbf{2}, \mathbf{2})_C$ Higgs is also present at the intermediate scale, it turns out that gauge coupling unification is still realized, with $\log_{10} M_{int} = 9.28$, $\log_{10} M_{GUT} = 16.38$, $\alpha_{GUT} = 0.038$, and $\log_{10} \tau_p(p \rightarrow e^+ \pi^0) = 35.9$. Here again, the mass scales and proton decay lifetime are expressed in units of GeV and

¹⁰For the effects of a $(\mathbf{15}, \mathbf{2}, \mathbf{2})_C$ Higgs field on the Yukawa couplings, see Refs. [27, 63].

years, respectively. Finally, we note that the addition of $(\mathbf{15}, \mathbf{2}, \mathbf{2})_C$ will not resurrect the failed models in Table 7.

4.3 Hypercharged DM

Hypercharged DM is a natural step forward after considering real triplet DM. In this section, we still restrict the Higgs content as in the previous section. As we discussed in Sec. 2.3, hypercharged DM is strongly constrained by direct detection experiments. To evade this constraint, we need to split the mass of the Weyl components of the hypercharged Dirac DM by ~ 100 keV. There are two possible ways to generate an effective operator in Eq. (3) through exchange of a field at the intermediate scale at tree level, depending on whether it is a scalar or a fermion. In the former case, the effective operator is induced by the exchange of intermediate-scale Higgs fields, as illustrated in Fig. 2(a). This requires the hypercharge of the virtual Higgs field to be at least one and $M_{\text{int}} \lesssim 10^9$ GeV. According to Table 6, the only candidate for such a Higgs field belongs to $(\mathbf{15}, \mathbf{1}, \mathbf{3})$ in the $\mathbf{210}$ when $G_{\text{int}} = \text{SU}(4)_C \otimes \text{SU}(2)_L \otimes \text{SU}(2)_R$. The DM candidate should then be in a $(\mathbf{15}, \mathbf{2}, \mathbf{2})$ or $(\overline{\mathbf{10}}, \mathbf{2}, \mathbf{2}) \oplus (\mathbf{10}, \mathbf{2}, \mathbf{2})$ representation of $\text{SU}(4)_C \otimes \text{SU}(2)_L \otimes \text{SU}(2)_R$. We performed a scan for models that contain above content, and found that none of them gives appropriate M_{int} and M_{GUT} . The latter possibility is to introduce another fermionic real multiplet at the intermediate scale, so that the DM candidate is a mixture of a hypercharged field and a Majorana field. This mechanism is demonstrated in Fig. 2(b), where R_{DM} is the main component of the DM candidate which is hypercharged and has a mass term of TeV scale; R'_{DM} is the Majorana field at the intermediate scale. The cross mark in Fig. 2(b) represents the chiral flipping in the propagator of the Majorana field R'_{DM} . R_{DM} and R'_{DM} couple to the SM Higgs field through terms like

$$\mathcal{L}_{\text{mix}} \propto \overline{R}_{\text{DM}} R'_{\text{DM}} R_H + \text{h.c.} \quad (12)$$

Since R'_{DM} is a Majorana field, it can only belong to either a singlet or a real triplet among the possible candidates in Table 2. As a result, DM can only belong to a doublet ($\mathbf{F}_2^{1/2}$ or $\widehat{\mathbf{F}}_2^{1/2}$) or a quartet ($\mathbf{F}_4^{1/2}$), with hypercharge 1/2. This requires $M_{\text{int}} \lesssim 10^9$ GeV according to the discussion in Sec. 2.3. Note that the $Y \geq 1$ DM candidates, \mathbf{F}_3^1 , $\widehat{\mathbf{F}}_3^1$, and $\mathbf{F}_4^{3/2}$, require at least $2Y$ additional fermions at the intermediate scale to generate the effective operator in Eq. (3). To minimize our model content, we do not consider these possibilities in the following discussion.

Taking the above discussion into account, we list the possible $\text{SO}(10)$ representations for R_{DM} in the upper part of Table 8; the singlet and real triplet candidates for R'_{DM} are listed in the lower part of Table 8 and Table 5, respectively. The quantum numbers of the DM candidates with respect to the intermediate gauge groups we consider can be inferred from the $\text{SU}(4)_C \otimes \text{SU}(2)_L \otimes \text{SU}(2)_R$ and $B - L$ quantum numbers listed in the table.

Now, we perform a one-loop calculation of M_{int} , M_{GUT} and the proton decay lifetime for various combination of R_{DM} , R'_{DM} and intermediate scale Higgs fields. Then, we pick up the models that are not yet ruled out by proton decay experiments, and at the same time have a relatively low intermediate scale $M_{\text{int}} \lesssim 10^9$. We also require that the models

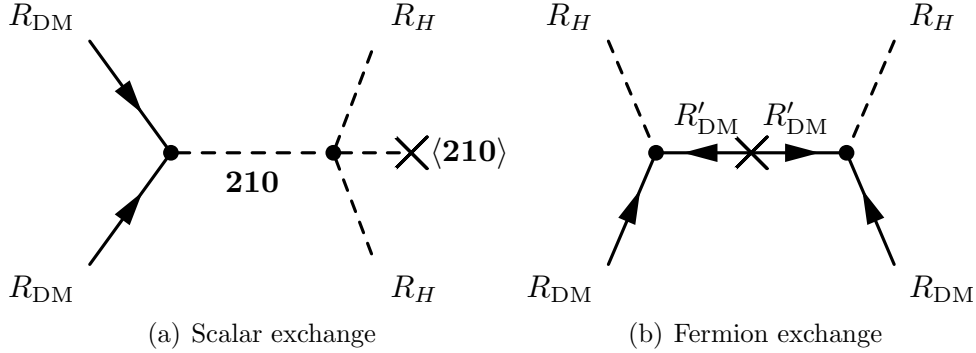


Figure 2: Diagrams that generate the mass splitting between the Weyl components of hypercharged Dirac DM through the exchange of an intermediate-scale (a) scalar (b) fermion.

Table 8: The upper half of the table shows the fermionic $Y = 1/2$ candidates for R_{DM} in various $SO(10)$ representations; the lower half of the table shows the fermionic singlet candidates for R'_{DM} .

SO(10) representation	$SU(4)_C \otimes SU(2)_L \otimes SU(2)_R$	$B - L$
10, 120, 210'	(1, 2, 2)	0
120, 126	(15, 2, 2)	0
210	(10, 2, 2) \oplus ($\overline{10}$, 2, 2)	± 2
210'	(1, 4, 4)	0
54, 210	(1, 1, 1)	0
45	(1, 1, 3)	0
45, 210	(15, 1, 1)	0
210	(15, 1, 3)	0
126	(10, 1, 3)	2

have appropriate particle and Higgs content, so that the DM acquires the right mass through Eq. (11) and Eq. (12). It turns out that the viable models are limited to $G_{\text{int}} = SU(4)_C \otimes SU(2)_L \otimes SU(2)_R$ or $SU(4)_C \otimes SU(2)_L \otimes U(1)_R$. These models are listed in Table 9 and no quartic models ($\mathbf{F}_4^{1/2}$) were found. The model \mathbf{FA}_{422} is incompatible with small neutrino masses, since the Yukawa coupling for the $\mathbf{16}$ of this model is unified at M_{GUT} . For models \mathbf{FA}_{421} and \mathbf{FB}_{422} , on the other hand, we can avoid the neutrino mass problem by fine-tuning the Yukawa couplings with additional Higgs fields at the intermediate scale, as discussed in Sec. 4.2. Among them, the model \mathbf{FA}_{421} has a phenomenologically interesting consequence. Since $M_{\text{int}} \simeq 3$ TeV, this model predicts a new massive neutral gauge

boson, Z' , and vector leptoquarks whose masses are around a few TeV. These particles can be probed in future LHC experiments; for instance, dilepton resonance searches [64] are powerful probes for such a Z' . The leptoquarks are pair produced at the LHC, and their signature is observed in dijet plus dilepton channels [65]. Since they are produced via the strong interaction, their production cross section is quite large. Thanks to the distinct final states and large production cross section, the LHC experiments can probe TeV-scale leptoquarks at the next stage of the LHC running.

Table 9: *Possible hypercharged fermionic DM models that is not yet excluded by current proton decay experiments. The quantum numbers are labeled in the same order as G_{int} . The subscripts D and W refer to Dirac and Weyl respectively. The numerical results are calculated for DM mass of 1 TeV. The mass scales and proton decay lifetime are in unit of GeV and years, respectively.*

Model	R_{DM}	R'_{DM}	Higgs	$\log_{10} M_{\text{int}}$	$\log_{10} M_{\text{GUT}}$	α_{GUT}	$\log_{10} \tau_p$
$G_{\text{int}} = \text{SU}(4)_C \otimes \text{SU}(2)_L \otimes \text{U}(1)_R$							
FA ₄₂₁	$(\mathbf{1}, \mathbf{2}, 1/2)_D$	$(\mathbf{15}, \mathbf{1}, 0)_W$	$(\mathbf{15}, \mathbf{1}, 0)_R$ $(\mathbf{15}, \mathbf{2}, 1/2)_C$	3.48	17.54	0.0320	40.9 ± 1.2
$G_{\text{int}} = \text{SU}(4)_C \otimes \text{SU}(2)_L \otimes \text{SU}(2)_R$							
FA ₄₂₂	$(\mathbf{1}, \mathbf{2}, \mathbf{2})_W$	$(\mathbf{1}, \mathbf{3}, \mathbf{1})_W$	$(\mathbf{15}, \mathbf{1}, \mathbf{1})_R$ $(\mathbf{15}, \mathbf{1}, \mathbf{3})_R$	9.00	15.68	0.0258	34.0 ± 1.2
FB ₄₂₂	$(\mathbf{1}, \mathbf{2}, \mathbf{2})_W$	$(\mathbf{1}, \mathbf{3}, \mathbf{1})_W$	$(\mathbf{15}, \mathbf{1}, \mathbf{1})_R$ $(\mathbf{15}, \mathbf{2}, \mathbf{2})_C$ $(\mathbf{15}, \mathbf{1}, \mathbf{3})_R$	5.84	17.01	0.0587	38.0 ± 1.2

To conclude this section, we perform a scan for more general models where the additional intermediate scale Higgs fields are not restricted to the ones in R_1 . Instead, they can be any combination of G_{int} representations that contain SM singlets. The Higgs fields can be taken to be either real or complex. Moreover, we also consider the possible addition of a $(\mathbf{15}, \mathbf{2}, \mathbf{2})_C$ Higgs at the intermediate scale, which can be used to evade the problem of large neutrino masses. The result of the scan is demonstrated in a scatter plot in Fig. 3. The DM mass is again fixed to be 1 TeV. The real triplet DM, $R_{\text{DM}}-R'_{\text{DM}}$ doublet-singlet mixing DM and doublet-triplet mixing DM cases are colored in red, blue and green, respectively. The triangle, circle and square marker corresponds to $G_{\text{int}} = \text{SU}(4)_C \otimes \text{SU}(2)_L \otimes \text{U}(1)_R$, $\text{SU}(4)_C \otimes \text{SU}(2)_L \otimes \text{SU}(2)_R$ and $\text{SU}(4)_C \otimes \text{SU}(2)_L \otimes \text{SU}(2)_R \otimes D$, respectively. The $M_{\text{int}} > M_{\text{GUT}}$ region is theoretically disfavored, and is indicated by the gray shaded area. In this plot, we do not consider the realizability of the mass hierarchy for the DM multiplet, and thus the number of good models should be smaller than that shown in the plot. All of the $\text{SU}(4)_C \otimes \text{SU}(2)_L \otimes \text{SU}(2)_R \otimes D$ cases with doublet DM predict the same M_{int} , since the addition of extra fields at the intermediate scale does not change M_{int} in the presence of the left-right symmetry [24]. As can be seen from the figure, model

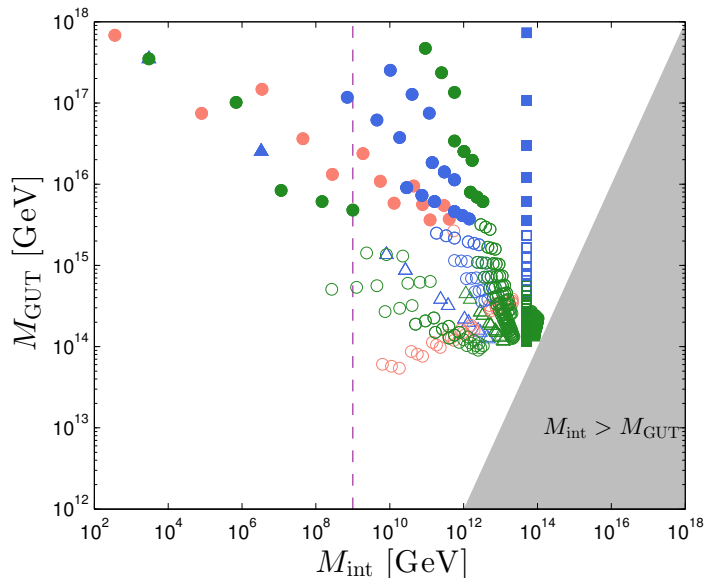


Figure 3: A scatter plot of general fermionic DM models. Here, the DM mass is set to be 1 TeV. The real triplet DM, doublet-singlet mixing DM and doublet-triplet mixing DM cases are colored in red, blue and green, respectively. The triangle, circle and square marker corresponds to $G_{int} = \text{SU}(4)_C \otimes \text{SU}(2)_L \otimes \text{U}(1)_R$, $\text{SU}(4)_C \otimes \text{SU}(2)_L \otimes \text{SU}(2)_R$ and $\text{SU}(4)_C \otimes \text{SU}(2)_L \otimes \text{SU}(2)_R \otimes D$, respectively. The vertical dashed line at 10^9 GeV indicates the direct detection constraint for $Y = 1/2$ dark matter. The gray shaded area is disfavored for $M_{int} > M_{GUT}$. Only the filled symbols are consistent with a sufficiently long proton lifetime.

points are concentrated in the high intermediate scale and low GUT scale region. After we apply the constraint of proton decay lifetime (shown by the filled symbols) as well as the condition $M_{int} \lesssim 10^9$ GeV for the doublet DM cases, the viable candidates turn out to be fairly limited.

4.4 Constraints and prospects for the fermion DM candidates

Finally, we review the present experimental constraints and future prospects of the fermionic DM candidates discussed in this section. Let us begin with the real triplet DM case. At the LHC, this DM candidate can be probed by searching for disappearing tracks caused by the charged component of the triplet DM, which has a decay length of $\mathcal{O}(1)$ cm. Such a small decay length is due to the small mass difference between the neutral and charged components; it is as small as a hundred MeV, since it is induced at loop level¹¹

¹¹Currently, the mass difference is computed at two-loop level [66]: for a 3-TeV triplet DM, the mass difference is about 165 MeV.

after electroweak symmetry breaking. Based on this search strategy, the ATLAS experiment has searched for triplet DM and has given a lower bound on the DM mass of $m_{\text{DM}} > 270$ GeV [67]. For future prospects on collider searches of triplet DM, see Ref. [68]. Indirect searches of triplet DM are also promising since this DM has a large annihilation cross section, as already seen in Sec. 4.1. Indeed, an excess of cosmic-ray antiprotons observed by the AMS-02 experiment [69] might be the first signature of triplet DM [70]. On the other hand, this DM is currently being constrained by the searches for gamma-ray line spectrum coming from the Galactic Center. As discussed in Ref. [71], the results from the H.E.S.S. Collaboration [72] may give a strong limit on triplet DM, though the consequences depend on the DM density profile used in the analysis. More robust constraints are obtained by means of the observation of gamma rays from dwarf spheroidal galaxies given by the Fermi-LAT collaboration [73]; according to that result, the mass of triplet DM is limited to $320 \text{ GeV} \leq m_{\text{DM}} \leq 2.25 \text{ TeV}$ and $2.43 \text{ TeV} \leq m_{\text{DM}}$ at 95% confidence level [74]. In the future, gamma-ray search experiments can probe a wider range of masses region for triplet DM. Direct detection experiments are also able to catch the signature of triplet DM. The scattering of triplet DM with a nucleon is induced by the exchange of the electroweak gauge bosons at loop level [75], and its scattering cross section is evaluated at the next-to-leading order in Ref. [76]: for instance, $\sigma_{\text{SI}} \simeq 2 \times 10^{-47} \text{ cm}^2$ for a 3 TeV real triplet DM, which is well above the neutrino background [77]. For relevant works, see also Ref. [78]. As a consequence, the triplet DM scenario can be tested in various future experiments, and therefore is a quite interesting possibility among the SO(10) DM candidates.

Next, we consider the doublet DM case. Contrary to triplet DM, doublet DM is rather hard to probe in experiments. In this case, the mass difference between the neutral and charged components is found to be as large as several hundreds of MeV, which makes it difficult to search for doublet DM signal events at the LHC by using the disappearing track method. The most promising way to probe doublet DM is the direct pair production at the ILC, which also enables us to study its properties precisely [79]. The indirect DM searches are also less promising due to a relatively small annihilation cross section of doublet DM. The direct detection of this DM is only possible when the intermediate scale is as low as 10^5 GeV [42]; in this case, the DM-nucleon scattering occurs through the exchange of the Higgs boson, which is induced by effective operators generated at the intermediate scale.¹² In addition, if there are additional CP phases in the effective operators, the electric dipole moment of electron is sensitive to the effects of doublet DM [41, 42]. For instance, the model FA_{421} and FB_{422} in Table 9 may be tested in these experiments. After all, the prospects for probing doublet DM quite depend on the intermediate scale, and future experiments are able to search for some of the doublet DM models discussed above.

¹²The electroweak loop contribution to the DM-nucleon scattering in this case turns out to be very small [76].

4.5 Non-thermal Hypercharged DM

In our previous discussion of fermionic hypercharged DM, we have assumed the DM to be in thermal equilibrium before freeze out so that the DM mass is restricted to be $\mathcal{O}(1 \text{ TeV})$ by the observed abundance. As a consequence, hypercharged DM is highly restricted by direct detection experiments. One way around such a constraint is to introduce a small mass splitting between the Weyl components of the DM by mixing the DM with another Majorana multiplet at the intermediate scale. On the other hand, as suggested in Ref. [48], non-thermally produced DM can be extremely heavy and thus avoid the direct detection constraint even when there is no mass splitting between the Weyl components. As a result, a minimal hypercharged DM model is possible in this scenario. This minimality motivates us to consider this class of DM candidates, even though they are not WIMPs.

First, let us derive the lower bound on the DM mass to evade the direct detection constraints. A fermionic DM particle with non-zero hypercharge Y scatters off a nucleus via the exchange of Z boson, and its scattering cross section is given by

$$\sigma = \frac{G_F^2 Y^2}{2\pi} [N - (1 - 4 \sin^2 \theta_W) Z]^2 \left(\frac{m_{\text{DM}} m_T}{m_{\text{DM}} + m_T} \right)^2, \quad (13)$$

where G_F is the Fermi constant, θ_W is the weak mixing angle, Z and N are the numbers of protons and neutrons in the nucleus, respectively, and m_T denotes the mass of the target nucleus. The LUX limit [59] then reads¹³

$$m_{\text{DM}} \gtrsim (2Y)^2 \times 6 \times 10^7 \text{ GeV}. \quad (14)$$

Such a heavy DM candidate can lead to the correct relic abundance if its mass is larger than the reheating temperature T_R after inflation so that it never reaches equilibrium with the thermal bath of SM particles. Then by carefully choosing the DM mass, the reheating temperature, and the maximum temperature after inflation, one obtains the desired relic abundance. The reheating temperature was shown to be in a range of [48]

$$T_R \simeq 10^{(7-9)} \left(\frac{m_{\text{DM}}}{3 \times 10^{10} \text{ GeV}} \right). \quad (15)$$

In this scenario, it is natural to assume the DM mass scale to be equal to intermediate scales of the unification models that we consider. Usually, M_{int} is large enough to evade the direct detection bound and yet not so large that gravitational production of DM becomes dominant. Moreover, we do not need to worry about mass splitting in the DM multiplet, as we did in the WIMP scenario. For such heavy particles, the electroweak and strong corrections to the masses of charged or colored particles in the multiplet are large enough to prevent them from acquiring cosmological lifetimes. This allows us to consider minimal hypercharged DM models, which contain only one DM multiplet without any extra Higgs multiplets with respect to the minimal SO(10) unification model.

¹³For ^{131}Xe target, $Z = 54$, $N = 77$.

The $Y = 1/2$ DM candidates we consider include those in the upper part of Table 8, and the $Y = 1$ candidates listed in Table 10. The last multiplet in the upper part of Table 8 also contains an $Y = 3/2$ candidate of DM which we will also consider. Now that the DM multiplet only contributes to the running above M_{int} , we will also consider the cases of $G_{\text{int}} = \text{SU}(3)_C \otimes \text{SU}(2)_L \otimes \text{SU}(2)_R \otimes \text{U}(1)_{B-L}$ and $\text{SU}(3)_C \otimes \text{SU}(2)_L \otimes \text{SU}(2)_R \otimes \text{U}(1)_{B-L} \otimes D$, in contrast to the WIMP scenario.

Table 10: *Fermionic $Y = 1$ candidates for R_{DM} in various $\text{SO}(10)$ representations;*

SO(10) representation	$\text{SU}(4)_C \otimes \text{SU}(2)_L \otimes \text{SU}(2)_R$	$B - L$
54	(1, 3, 3)	0
126	(10, 3, 1)	2

After an exhaustive calculation for different choices of R_{DM} and G_{int} , we find several possible models listed in Table 11 that survive the direct detection and proton decay constraints. Viable minimal models only exist for doublet DM when $G_{\text{int}} = \text{SU}(4)_C \otimes \text{SU}(2)_L \otimes \text{SU}(2)_R$, $G_{\text{int}} = \text{SU}(4)_C \otimes \text{SU}(2)_L \otimes \text{SU}(2)_R \otimes D$ and $G_{\text{int}} = \text{SU}(3)_C \otimes \text{SU}(2)_L \otimes \text{SU}(2)_R \otimes \text{U}(1)_{B-L}$. The intermediate scale of each model is larger than 10^8 GeV, large enough to evade the direct detection bound indicated by Eq. (14). As can be seen, most of the models in Table 11 can be probed in future proton decay experiments, though it is hard to detect these DM candidates in direct detection experiments.

Table 11: *Possible non-thermal hypercharged fermionic DM models that are not yet excluded by current direct detection and proton decay experiments. The quantum numbers are labeled in the same order as G_{int} . The numerical results are calculated for DM mass equal to M_{int} . The mass scales and proton decay lifetimes are in unit of GeV and years, respectively.*

Model	R_{DM}	$\log_{10} M_{\text{int}}$	$\log_{10} M_{\text{GUT}}$	α_{GUT}	$\log_{10} \tau_p$
$G_{\text{int}} = \text{SU}(4)_C \otimes \text{SU}(2)_L \otimes \text{SU}(2)_R$					
FNA ₄₂₂	(1, 2, 2)_W	12.10	15.63	0.0225	34.0 ± 1.2
FNB ₄₂₂	(15, 2, 2)_W	11.15	16.77	0.0387	37.9 ± 1.2
$G_{\text{int}} = \text{SU}(4)_C \otimes \text{SU}(2)_L \otimes \text{SU}(2)_R \otimes D$					
FNA _{422D}	(15, 2, 2)_W	13.71	15.36	0.0286	32.8 ± 1.2
FNB _{422D}	(10, 2, 2)_D	13.71	15.94	0.0342	34.9 ± 1.2
$G_{\text{int}} = \text{SU}(3)_C \otimes \text{SU}(2)_L \otimes \text{SU}(2)_R \otimes \text{U}(1)_{B-L}$					
FNA ₃₂₂₁	(1, 2, 2, 0)_W	10.34	15.82	0.0227	34.8 ± 1.2

5 Conclusion and discussion

The success of the Standard Model is now well established. Nevertheless, we know that the Standard Model is incomplete. Neutrinos have masses, there is a non-zero baryon asymmetry in the Universe, and dark matter makes up a sizable component of the total matter density. Many extensions to the Standard Model have been studied to explain these phenomena. But rarely can a single extension explain all three. SO(10) grand unification is one such example.

In most models, SO(10) symmetry breaking involves an intermediate gauge group, whose unknown scale presumably lies between the weak scale and the grand unified scale (defined by the renormalization scale where the gauge couplings are equal). Standard Model fermions are neatly contained in a **16** of SO(10) which includes all of the known SM fermions plus a right-handed neutrino per generation. As the right-handed neutrino is a SM singlet, it easily picks up a mass of order the intermediate scale during the second phase of symmetry breaking, and leads to a natural realization of the see-saw mechanism [22] for the generation of neutrino masses. If produced (thermally or non-thermally) after inflation, these same right-handed neutrinos can decay out of equilibrium and produce a lepton asymmetry which can be converted through electroweak effects to a baryon asymmetry, a process known as leptogenesis [80]. Furthermore the existence of an intermediate scale makes gauge coupling unification feasible in the absence of supersymmetry.

Here we studied in detail one of the often unheralded features of SO(10) grand unification. Namely its ability to provide for a WIMP dark matter candidate in addition to the benefits described above. Since SO(10) includes an additional U(1) symmetry beyond hypercharge, if the Higgs field that breaks this symmetry at the intermediate scale belongs to a **126** dimensional representation, then a discrete \mathbb{Z}_2 symmetry is preserved at low energies. This discrete symmetry (equivalent to matter parity $P_M = (-1)^{3(B-L)}$) naturally provides the stability for dark matter candidates. We considered all possible intermediate gauge group with broken SU(5).

Stable SO(10) scalar (fermion) DM candidates must be odd (even) under the \mathbb{Z}_2 symmetry. Therefore fermions must originate in either a **10**, **45**, **54**, **120**, **126**, **210** or **210'** representation, while scalars are restricted to either a **16** or **144** of SO(10). These multiplets must be split and we gave explicit examples of fine-tuning mechanisms in order to retain a 1 TeV WIMP candidate which may be a SU(2)_L singlet, doublet, triplet, or quartet with or without hypercharge. Fermions which are SU(2)_L singlets with no hypercharge are not good WIMP candidates but are NETDM candidates and these were considered elsewhere [24]. Our criteria for a viable dark matter model required: gauge coupling unification at a sufficiently high scale to ensure proton stability compatible with experiment; a unification scale greater than the intermediate scale; and elastic cross sections compatible with direct detection experiments. The latter criterion often requires additional Higgs representations to split the degeneracy of the fermionic intermediate scale representations if DM is hypercharged.

Despite the potential very long list of candidates (when one combines the possible different SO(10) representations and intermediate gauge groups), we found only a handful

of models which satisfied all constraints. Among the scalar candidates, the $Y = 0$ singlet and $Y = 1/2$ doublet (often referred to as an inert Higgs doublet [50]) are possible candidates for $SU(4)_C \otimes SU(2)_L \otimes SU(2)_R$ and $SU(3)_C \otimes SU(2)_L \otimes SU(2)_R \otimes U(1)_{B-L}$ (with or without a left-right symmetry) intermediate gauge groups. These originate from either the **16** or **144** of $SO(10)$. The latter group (without the left-right symmetry) is also consistent with a state originating from the **144** being a triplet under $SU(2)_R$. To avoid immediate exclusion from direct detection experiments, a mass splitting of order 100 keV implies that the intermediate scale must be larger than about $3 \times 10^{-6} M_{\text{GUT}}$ for a nominal 1 TeV hypercharged scalar DM particle. Some of these models imply proton lifetimes short enough to be testable in on-going and future proton decay experiments.

The fermion candidates were even more restrictive. Models with $Y = 0$ must come from a $SU(2)_L$ triplet (singlets are not WIMPs). In this case only one model was found using the $SU(4)_C \otimes SU(2)_L \otimes SU(2)_R$ intermediate gauge group and requiring additional Higgses (already present in R_1) at the intermediate scale. Models with $Y = 1/2$ doublets were found for $SU(4)_C \otimes SU(2)_L \otimes U(1)_R$ with a singlet fermion required for mixing, and $SU(4)_C \otimes SU(2)_L \otimes SU(2)_R$ with a triplet fermion for mixing. In both cases, additional Higgses from R_1 are required at the intermediate scale. More possibilities can be found if the additional Higgs are taken outside R_1 .

$SO(10)$ almost always involves rather large representations (at least when compared with minimal $SU(5)$ for example). $SO(10)$ itself can be broken by either a **45**, **54** or **210** representation (R_1) which determines the intermediate scale gauge group and a **126** is needed to break down to the SM (and preserve the needed \mathbb{Z}_2 symmetry). The SM Higgs originates from a **10** and matter fields reside in three copies of **16**'s. One additional representation is needed to account for DM. We have delineated the possible representations and necessary intermediate gauge groups needed to account for WIMP-like dark matter, proton stability, and gauge coupling unification. Some of these models are accessible for experimental tests.

Acknowledgments

We thank Yann Mambrini and Mikhail B. Voloshin for valuable discussions. The work of N.N. is supported by Research Fellowships of the Japan Society for the Promotion of Science for Young Scientists. The work of K.A.O. was supported in part by DOE grant de-sc0011842 at the University of Minnesota.

Appendix

A Dark matter candidates in $SO(10)$

Here we give a group theoretical argument to classify possible DM candidates in $SO(10)$ models. We basically follow the notation of Ref. [36] in the following discussion. See also

Refs. [23, 24].

Since $\text{SO}(10)$ is a rank-five group, we have five linearly independent Cartan generators. We denote them by H_i ($i = 1, \dots, 5$). In the dual basis, they are expressed in terms of five-dimensional vectors as follows:

$$\begin{aligned} H_1 &= \frac{1}{2}[1 \ 2 \ 2 \ 1 \ 1] , \\ H_2 &= \frac{1}{2\sqrt{3}}[1 \ 0 \ 0 \ -1 \ 1] , \\ H_3 &= \frac{1}{2}[0 \ 0 \ 1 \ 1 \ 1] , \\ H_4 &= \frac{1}{6}[-2 \ 0 \ 3 \ -1 \ 1] , \\ H_5 &= [2 \ 0 \ 2 \ 1 \ -1] . \end{aligned} \tag{16}$$

Here, H_1 and H_2 are the $\text{SU}(3)_C$ Cartan generators. H_3 and H_4 are the weak isospin and hypercharge, T_{3L} and Y , respectively. H_5 is given by $H_5 = -5(B - L) + 4Y$.

Every component of an $\text{SO}(10)$ multiplet is specified by a weight vector $\boldsymbol{\mu}$, which is expressed by a set of five integers called Dynkin labels as $\boldsymbol{\mu} = (\tilde{\mu}_1, \dots, \tilde{\mu}_5)$. Its eigenvalues of H_i are given by

$$H_i(\boldsymbol{\mu}) = \sum_{j=1}^5 \bar{h}_{ij} \tilde{\mu}_j , \tag{17}$$

with $H_i = [\bar{h}_{i1}, \dots, \bar{h}_{i5}]$.

The DM particle should have zero eigenvalues of H_1 , H_2 , and $Q = H_3 + H_4$. This condition is satisfied by the following set of weight vectors characterized by two integers N and M :

$$\boldsymbol{\mu}_{N,M} = (-N \ N \ -M \ -N + M \ M) . \tag{18}$$

The hypercharge and $B - L$ charge of the weight vector are

$$Y(\boldsymbol{\mu}_{N,M}) = \frac{1}{2}(N - M) , \quad B - L(\boldsymbol{\mu}_{N,M}) = N . \tag{19}$$

We find that the $N \neq M$ cases correspond to the hypercharged DM candidates. For $N = M$, the weight vector agrees to $\boldsymbol{\mu}_N$ discussed in Ref. [24].

A convenient way to determine the matter parity of the DM candidates $\boldsymbol{\mu}_{N,M}$ is to consider congruence classes of $\text{SO}(10)$ [36]. Two representations R and R' of $\text{SO}(10)$ belong to the same congruence class if the difference between any weights of R and R' is always written as a linear combination of simple roots of $\text{SO}(10)$ with integer coefficients [81]. $\text{SO}(10)$ has four congruence classes. Each congruence class is characterized by a congruence number. The congruence number of a weight vector $\boldsymbol{\mu} = (\tilde{\mu}_1, \dots, \tilde{\mu}_5)$ is defined by

$$c(\boldsymbol{\mu}) \equiv 2\tilde{\mu}_1 + 2\tilde{\mu}_3 - \tilde{\mu}_4 + \tilde{\mu}_5 \pmod{4} . \tag{20}$$

For $\mu_{N,M}$, we thus have

$$c(\mu_{N,M}) \equiv 3N + 2M \pmod{4} . \quad (21)$$

Then, we find that the congruence number of $\mu_{N,M}$ is ± 1 if and only if N is an odd integer. Considering Eq. (19), we conclude that a DM particle has the odd matter parity if it has a congruence number of ± 1 , while it has the even matter parity if its congruence number is 0 or 2.

B Proton decay calculation

In this section, we describe how we calculate proton decay lifetimes in the intermediate-scale scenarios. In these scenarios, proton decay is induced by the exchange of the GUT-scale gauge bosons [82]. The relevant part of the SO(10) gauge interaction is given by

$$\mathcal{L}_{\text{int}} = \frac{g_{\text{GUT}}}{\sqrt{2}} [(\bar{Q})_{ar} X^{air} P_R(L^c)_i + (\bar{Q})_{ai} X^{air} P_L(L^c)_r + \epsilon_{ij} \epsilon_{rs} \epsilon_{abc} (\bar{Q}^c)^{ar} X^{bis} P_L Q^{cj} + \text{h.c.}] , \quad (22)$$

where

$$Q = \begin{pmatrix} u \\ d \end{pmatrix} , \quad L = \begin{pmatrix} \nu \\ e^- \end{pmatrix} , \quad (23)$$

X represents the GUT gauge bosons which induce proton decay, g_{GUT} is the unified gauge coupling constant, a, b, c are $\text{SU}(3)_C$ indices, i, j are $\text{SU}(2)_L$ indices, r, s are $\text{SU}(2)_R$ indices, and $P_{R/L} \equiv (1 \pm \gamma_5)/2$ are the chirality projection operators. The exchange of the X fields generates dimension-six proton decay operators. These operators are expressed in a form that respects the intermediate gauge symmetries. Between the GUT and intermediate scales, the renormalization factors for the effective operators are in general different among the choices of G_{int} . Below the intermediate scale, the low-energy effective theory is described by the $\text{SU}(3)_C \otimes \text{SU}(2)_L \otimes \text{U}(1)_Y$ gauge theory, and thus after matching the theories above and below the intermediate scale, the prescription for the calculation is common to all of the cases. For this reason, we first describe the calculation below the intermediate scale. After that, we discuss each intermediate gauge theory showing the matching conditions at the GUT and intermediate scales as well as the RGEs between them.

In the $\text{SU}(3)_C \otimes \text{SU}(2)_L \otimes \text{U}(1)_Y$ gauge theory, the effective Lagrangian for proton decay is generically written as

$$\mathcal{L}_{\text{eff}} = \sum_{I=1}^4 C_I \mathcal{O}_I + \text{h.c.} , \quad (24)$$

with the effective operators given by [83–85]

$$\begin{aligned}
\mathcal{O}_1 &= \epsilon_{abc}\epsilon_{ij}(u_R^a d_R^b)(Q_L^{ci} L_L^j) , \\
\mathcal{O}_2 &= \epsilon_{abc}\epsilon_{ij}(Q_L^{ai} Q_L^{bj})(u_R^c e_R) , \\
\mathcal{O}_3 &= \epsilon_{abc}\epsilon_{ij}\epsilon_{kl}(Q_L^{ai} Q_L^{bk})(Q_L^{cl} L_L^j) , \\
\mathcal{O}_4 &= \epsilon_{abc}(u_R^a d_R^b)(u_R^c e_R) ,
\end{aligned} \tag{25}$$

up to dimension six. We then run down the coefficients to the electroweak scale. We will see below that the coefficients C_3 and C_4 vanish in all of the cases we consider in this paper, and thus we focus on C_1 and C_2 . Their renormalization factors are [85]

$$C_1(\mu) = \left[\frac{\alpha_3(\mu)}{\alpha_3(M_{\text{int}})} \right]^{-\frac{2}{b_3}} \left[\frac{\alpha_2(\mu)}{\alpha_2(M_{\text{int}})} \right]^{-\frac{9}{4b_2}} \left[\frac{\alpha_1(\mu)}{\alpha_1(M_{\text{int}})} \right]^{-\frac{11}{20b_1}} C_1(M_{\text{int}}) , \tag{26}$$

$$C_2(\mu) = \left[\frac{\alpha_3(\mu)}{\alpha_3(M_{\text{int}})} \right]^{-\frac{2}{b_3}} \left[\frac{\alpha_2(\mu)}{\alpha_2(M_{\text{int}})} \right]^{-\frac{9}{4b_2}} \left[\frac{\alpha_1(\mu)}{\alpha_1(M_{\text{int}})} \right]^{-\frac{23}{20b_1}} C_2(M_{\text{int}}) , \tag{27}$$

where b_a denote the one-loop beta-function coefficients for the gauge couplings g_a and μ is an arbitrary scale. We need to change the beta-function coefficients appropriately when we across the DM mass threshold. Below the electroweak scale, the QCD corrections are the dominant contribution. By using the two-loop RGE given in Ref. [86], we compute the Wilson coefficients at the hadronic scale μ_{had} as

$$C_i(\mu_{\text{had}}) = \left[\frac{\alpha_s(\mu_{\text{had}})}{\alpha_s(m_b)} \right]^{\frac{6}{25}} \left[\frac{\alpha_s(m_b)}{\alpha_s(m_Z)} \right]^{\frac{6}{23}} \left[\frac{\alpha_s(\mu_{\text{had}}) + \frac{50\pi}{77}}{\alpha_s(m_b) + \frac{50\pi}{77}} \right]^{-\frac{173}{825}} \left[\frac{\alpha_s(m_b) + \frac{23\pi}{29}}{\alpha_s(m_Z) + \frac{23\pi}{29}} \right]^{-\frac{430}{2001}} C_i(m_Z) , \tag{28}$$

with $i = 1, 2$.

In non-SUSY GUTs, the dominant decay mode of proton is $p \rightarrow \pi^0 e^+$. The partial decay width of the mode is computed as

$$\Gamma(p \rightarrow \pi^0 e^+) = \frac{m_p}{32\pi} \left(1 - \frac{m_\pi^2}{m_p^2} \right)^2 [|\mathcal{A}_L|^2 + |\mathcal{A}_R|^2] , \tag{29}$$

where m_p and m_π are the masses of the proton and the neutral pion, respectively, and

$$\begin{aligned}
\mathcal{A}_L &= C_1(\mu_{\text{had}}) \langle \pi^0 | (ud)_R u_L | p \rangle , \\
\mathcal{A}_R &= 2C_2(\mu_{\text{had}}) \langle \pi^0 | (ud)_L u_R | p \rangle .
\end{aligned} \tag{30}$$

The hadron matrix elements are evaluated with the lattice QCD simulations in Ref. [87]. We have

$$\langle \pi^0 | (ud)_R u_L | p \rangle = \langle \pi^0 | (ud)_L u_R | p \rangle = -0.103(23)(34) \text{ GeV}^2 , \tag{31}$$

with $\mu_{\text{had}} = 2 \text{ GeV}$. Here, the first and second parentheses indicate statistical and systematic errors, respectively.

B.1 $G_{\text{int}} = \text{SU}(4)_C \otimes \text{SU}(2)_L \otimes \text{SU}(2)_R (\otimes D)$

For $G_{\text{int}} = \text{SU}(4)_C \otimes \text{SU}(2)_L \otimes \text{SU}(2)_R (\otimes D)$, the dimension-six effective operator is given by¹⁴

$$\mathcal{L}_{\text{eff}} = C_{422} \cdot \epsilon_{ij} \epsilon_{rs} \epsilon_{\alpha\beta\gamma\delta} (\overline{\Psi^C})^{\alpha i} P_L \Psi^{\beta j} (\overline{\Psi^C})^{\gamma r} P_R \Psi^{\delta s} + \text{h.c.} , \quad (33)$$

where α, β, \dots denote the $\text{SU}(4)$ indices, and the Dirac field $\Psi = (\Psi_L, \Psi_R)$ is defined by

$$\Psi_L = \begin{pmatrix} u_L^1 & u_L^2 & u_L^3 & \nu_L \\ d_L^1 & d_L^2 & d_L^3 & e_L \end{pmatrix} , \quad \Psi_R^C = \begin{pmatrix} d_{R1}^C & d_{R2}^C & d_{R3}^C & e_R^C \\ -u_{R1}^C & -u_{R2}^C & -u_{R3}^C & -\nu_R^C \end{pmatrix} . \quad (34)$$

Here, the indices represent the $\text{SU}(3)_C$ color and C indicates charge conjugation. At tree level, the coefficient of the effective operator is evaluated as¹⁵

$$C_{422}(M_{\text{GUT}}) = -\frac{g_{\text{GUT}}^2}{2M_X^2} , \quad (35)$$

with M_X the mass of the heavy gauge field X . In this paper, we neglect fermion flavor mixings [88] for simplicity.

The Wilson coefficient is evolved down to the intermediate scale using the RGE. The renormalization factor is computed to be [89]

$$C_{422}(M_{\text{int}}) = \left[\frac{\alpha_4(M_{\text{int}})}{\alpha_{\text{GUT}}} \right]^{-\frac{15}{4b_4}} \left[\frac{\alpha_{2L}(M_{\text{int}})}{\alpha_{\text{GUT}}} \right]^{-\frac{9}{4b_{2L}}} \left[\frac{\alpha_{2R}(M_{\text{int}})}{\alpha_{\text{GUT}}} \right]^{-\frac{9}{4b_{2R}}} C_{422}(M_{\text{GUT}}) . \quad (36)$$

Then, the effective operator is matched onto the operators in Eq. (25). The Wilson coefficients C_I are given by¹⁶

$$\begin{aligned} C_1(M_{\text{int}}) &= 4C_{422}(M_{\text{int}}) , \\ C_2(M_{\text{int}}) &= 2C_{422}(M_{\text{int}}) , \\ C_3(M_{\text{int}}) &= C_4(M_{\text{int}}) = 0 . \end{aligned} \quad (37)$$

B.2 $G_{\text{int}} = \text{SU}(4)_C \otimes \text{SU}(2)_L \otimes \text{U}(1)_R$

In the case of $G_{\text{int}} = \text{SU}(4)_C \otimes \text{SU}(2)_L \otimes \text{U}(1)_R$, the effective Lagrangian is written as

$$\mathcal{L}_{\text{eff}} = C_{421} \cdot 2\epsilon_{ij} \epsilon_{\alpha\beta\gamma\delta} (\overline{\Psi^C})^{\alpha i} P_L \Psi^{\beta j} (\overline{\mathcal{U}^C})^{\gamma} P_R \mathcal{D}^{\delta} + \text{h.c.} , \quad (38)$$

¹⁴ Note that

$$\epsilon_{ij} \epsilon_{kl} \epsilon_{\alpha\beta\gamma\delta} (\overline{\Psi^C})^{\alpha i} P_L \Psi^{\beta j} (\overline{\Psi^C})^{\gamma k} P_L \Psi^{\delta l} = \epsilon_{rs} \epsilon_{tu} \epsilon_{\alpha\beta\gamma\delta} (\overline{\Psi^C})^{\alpha r} P_R \Psi^{\beta s} (\overline{\Psi^C})^{\gamma t} P_R \Psi^{\delta u} = 0 , \quad (32)$$

and thus the operator in Eq. (33) is the unique choice.

¹⁵We have found that the sign of this equation is opposite to that given in Ref. [24].

¹⁶We have fixed an error in the matching conditions given in Ref. [24].

with

$$\mathcal{U} \equiv (u^1, u^2, u^3, \nu), \quad \mathcal{D} \equiv (d^1, d^2, d^3, e). \quad (39)$$

The GUT-scale matching condition for the operator is

$$C_{421}(M_{\text{GUT}}) = -\frac{g_{\text{GUT}}^2}{2M_X^2}, \quad (40)$$

and the renormalization factor is given by [89]

$$C_{421}(M_{\text{int}}) = \left[\frac{\alpha_4(M_{\text{int}})}{\alpha_{\text{GUT}}} \right]^{-\frac{15}{4b_4}} \left[\frac{\alpha_{2L}(M_{\text{int}})}{\alpha_{\text{GUT}}} \right]^{-\frac{9}{4b_{2L}}} \left[\frac{\alpha_R(M_{\text{int}})}{\alpha_{\text{GUT}}} \right]^{-\frac{3}{4b_R}} C_{421}(M_{\text{GUT}}). \quad (41)$$

For the intermediate-scale matching conditions, we have

$$\begin{aligned} C_1(M_{\text{int}}) &= 4C_{421}(M_{\text{int}}), \\ C_2(M_{\text{int}}) &= 2C_{421}(M_{\text{int}}), \\ C_3(M_{\text{int}}) &= C_4(M_{\text{int}}) = 0. \end{aligned} \quad (42)$$

B.3 $G_{\text{int}} = \mathbf{SU}(3)_C \otimes \mathbf{SU}(2)_L \otimes \mathbf{SU}(2)_R \otimes \mathbf{U}(1)_{B-L} (\otimes D)$

When $G_{\text{int}} = \mathbf{SU}(3)_C \otimes \mathbf{SU}(2)_L \otimes \mathbf{SU}(2)_R \otimes \mathbf{U}(1)_{B-L} (\otimes D)$, there are four independent effective operators [90],

$$\begin{aligned} \mathcal{Q}_1 &= 2\epsilon_{ij}\epsilon_{rs}\epsilon_{abc}(\overline{Q^c})^{ai}P_LQ^{bj}(\overline{Q^c})^{cr}P_RL^s, \\ \mathcal{Q}_2 &= 2\epsilon_{ij}\epsilon_{rs}\epsilon_{abc}(\overline{Q^c})^{ai}P_LL^j(\overline{Q^c})^{br}P_RQ^{cs}, \\ \mathcal{Q}_3 &= 2\epsilon_{il}\epsilon_{jk}\epsilon_{abc}(\overline{Q^c})^{ai}P_LQ^{bj}(\overline{Q^c})^{ck}P_LL^l, \\ \mathcal{Q}_4 &= 2\epsilon_{ps}\epsilon_{qr}\epsilon_{abc}(\overline{Q^c})^{ap}P_RQ^{bq}(\overline{Q^c})^{cr}P_RL^s, \end{aligned} \quad (43)$$

and thus the effective Lagrangian is expressed as

$$\mathcal{L}_{\text{eff}} = \sum_{I=1}^4 C_{3221}^{(I)} \mathcal{Q}_I + \text{h.c.} \quad (44)$$

For the GUT-scale matching condition, we have

$$\begin{aligned} C_{3221}^{(1)}(M_{\text{GUT}}) &= C_{3221}^{(2)}(M_{\text{GUT}}) = -\frac{g_{\text{GUT}}^2}{2M_X^2}, \\ C_{3221}^{(3)}(M_{\text{GUT}}) &= C_{3221}^{(4)}(M_{\text{GUT}}) = 0. \end{aligned} \quad (45)$$

The renormalization factors for the coefficients $C_{3221}^{(1)}$ and $C_{3221}^{(2)}$ are given in Refs. [89, 90]:

$$\frac{C(M_{\text{int}})}{C(M_{\text{GUT}})} = \left[\frac{\alpha_3(M_{\text{int}})}{\alpha_{\text{GUT}}} \right]^{-\frac{2}{b_3}} \left[\frac{\alpha_{2L}(M_{\text{int}})}{\alpha_{\text{GUT}}} \right]^{-\frac{9}{4b_{2L}}} \left[\frac{\alpha_{2R}(M_{\text{int}})}{\alpha_{\text{GUT}}} \right]^{-\frac{9}{4b_{2R}}} \left[\frac{\alpha_{B-L}(M_{\text{int}})}{\alpha_{\text{GUT}}} \right]^{-\frac{1}{4b_{B-L}}}, \quad (46)$$

for $C = C_{3221}^{(1)}$ and $C_{3221}^{(2)}$. Then the Wilson coefficients at the electroweak scale are matched onto those of the operators (25) as

$$\begin{aligned} C_1(M_{\text{int}}) &= 4C_{3221}^{(2)}(M_{\text{int}}) , \\ C_2(M_{\text{int}}) &= 2C_{3221}^{(1)}(M_{\text{int}}) , \\ C_3(M_{\text{int}}) &= C_4(M_{\text{int}}) = 0 . \end{aligned} \tag{47}$$

C Example of fine-tuning

To show the process of mass fine-tuning explicitly, in this section, we consider the case of $R_{\text{DM}} = \mathbf{16}$ with $G_{\text{int}} = \text{SU}(3)_C \otimes \text{SU}(2)_L \otimes \text{SU}(2)_R \otimes \text{U}(1)_{B-L}$ as an example. We take $R_1 = \mathbf{45}$, which contains two independent SM singlet components that might develop VEVs; one is in a $(\mathbf{1}, \mathbf{1}, \mathbf{3})$ while the other is in a $(\mathbf{15}, \mathbf{1}, \mathbf{1})$ under $\text{SU}(4)_C \otimes \text{SU}(2)_L \otimes \text{SU}(2)_R$. We refer to these VEVs as A_1 and A_2 , respectively, and other notation is taken from Eq. (7). Since the components of a scalar $\mathbf{16}$ have the same quantum numbers as those of a generation of the SM fermions, we denote them by the same symbol as for the corresponding SM fermions with a tilde, just like the notation for sfermions in supersymmetric models.

Let us first study the $R_{\text{DM}}^* R_{\text{DM}} R_1$ coupling. Since R_1 is the adjoint representation of $\text{SO}(10)$, the decomposition of this coupling in terms of the component fields has a similar form to the gauge interaction for a $\mathbf{16}$ spinor representation. We have

$$\begin{aligned} \kappa_1 R_{\text{DM}}^* R_{\text{DM}} \langle R_1 \rangle &= \kappa_1 \left[\left(-\sqrt{2}A_1 - \sqrt{3}A_2 \right) \tilde{\nu}_R^* \tilde{\nu}_R + \left(\sqrt{2}A_1 - \sqrt{3}A_2 \right) \tilde{e}_R^* \tilde{e}_R + \sqrt{3}A_2 \tilde{L}_L^* \tilde{L}_L \right. \\ &\quad \left. + \left(\sqrt{2}A_1 + \frac{1}{\sqrt{3}}A_2 \right) \tilde{d}_R^* \tilde{d}_R + \left(-\sqrt{2}A_1 + \frac{1}{\sqrt{3}}A_2 \right) \tilde{u}_R^* \tilde{u}_R - \frac{1}{\sqrt{3}}A_2 \tilde{Q}_L^* \tilde{Q}_L \right] , \end{aligned} \tag{48}$$

where the contraction of the $\text{SU}(3)_C$ and $\text{SU}(2)_L$ indices is implicit. When $A_1 \neq 0$ and $A_2 = 0$, the mass spectrum preserves the $\text{SU}(4)_C \otimes \text{SU}(2)_L \otimes \text{U}(1)_R$ symmetry, while when $A_2 \neq 0$ and $A_1 = 0$, then it is $\text{SU}(3)_C \otimes \text{SU}(2)_L \otimes \text{SU}(2)_R \otimes \text{U}(1)_{B-L}$ symmetric. If both of the VEVs have non-zero values, then the low-energy theory is invariant under the $\text{SU}(3)_C \otimes \text{SU}(2)_L \otimes \text{U}(1)_R \otimes \text{U}(1)_{B-L}$ symmetry. The coefficients of A_2 for left and right doublets have different signs, which indicates the breaking of left-right symmetry. Here, we choose $A_1 = 0$ and $A_2 = v_{\mathbf{45}}$ to obtain $G_{\text{int}} = \text{SU}(3)_C \otimes \text{SU}(2)_L \otimes \text{SU}(2)_R \otimes \text{U}(1)_{B-L}$.

Next we consider the mass terms generated by $\lambda_2^{\mathbf{45}} (R_{\text{DM}}^* R_{\text{DM}})_{\mathbf{45}} (R_2^* R_2)_{\mathbf{45}}$. The SM singlet in $R_2 = \mathbf{126}$ transforms as $(\mathbf{10}, \mathbf{1}, \mathbf{3})$ under $\text{SU}(4)_C \otimes \text{SU}(2)_L \otimes \text{SU}(2)_R$, which acquires a VEV $v_{\mathbf{126}}$ to break G_{int} into the SM gauge group. According to the result in

Ref. [91], the resultant mass terms are¹⁷

$$\lambda_2^{45} (R_{\text{DM}}^* R_{\text{DM}})_{45} \langle (R_2^* R_2)_{45} \rangle = \lambda_2^{45} v_{126}^2 \left[-\tilde{\nu}_R^* \tilde{\nu}_R + \frac{3}{5} \left(\tilde{L}_L^* \tilde{L}_L + \tilde{d}_R^* \tilde{d}_R \right) - \frac{1}{5} \left(\tilde{e}_R^* \tilde{e}_R + \tilde{u}_R^* \tilde{u}_R + \tilde{Q}_L^* \tilde{Q}_L \right) \right]. \quad (49)$$

Notice that the right-hand side of the expression can be grouped in terms of SU(5) multiplets. This is expected since v_{126} is invariant under the SU(5) transformation. From the above equations, it is found that we can ensure that only the DM component has a mass around TeV scale by fine-tuning the parameters M^2 , κ_1 and λ_2^{45} . For example, to obtain the model SA_{3221} , we can take

$$\begin{aligned} M^2 - \sqrt{3}\kappa_1 v_{45} &\sim \mathcal{O}(M_{\text{int}}^2), \\ M^2 - \sqrt{3}\kappa_1 v_{45} - \lambda_2^{45} v_{126}^2 &\sim \mathcal{O}(\text{TeV}^2). \end{aligned} \quad (50)$$

Then, $\tilde{\nu}_R$ acquires a TeV-scale mass, while the mass of \tilde{e}_R is $\mathcal{O}(M_{\text{int}})$. The rest of the components lie around the GUT scale. On the other hand, if we take

$$\begin{aligned} M^2 + \sqrt{3}\kappa_1 v_{45} &\sim \mathcal{O}(M_{\text{int}}^2), \\ M^2 + \sqrt{3}\kappa_1 v_{45} + \frac{3}{5}\lambda_2^{45} v_{126}^2 &\sim \mathcal{O}(\text{TeV}^2), \end{aligned} \quad (51)$$

then we can make only the \tilde{L}_L component have a TeV-scale mass and the other components have GUT-scale masses. Thus we obtain the SB_{3221} model.

To simplify our argument, in the above discussion, we have taken into account only the contribution of the M^2 , κ_1 , and λ_2^{45} terms, and neglected that of the other terms in Eq. (7). Even in the presence of the other contributions, we can always perform a similar fine-tuning among the parameters to realize desired mass spectrum for our DM models.

¹⁷Note that since $(R_2^* R_2)_{45}$ contains a $\mathbf{45}$, there is a contribution to the mass corresponding to Eq. (48) at the intermediate scale proportional to λ_2^{45} with independent coefficients \tilde{A}_1 and \tilde{A}_2 . The result shown is obtained from Eq. (48) by taking $\tilde{A}_1 = \frac{\sqrt{2}}{5} v_{126}^2$ and $\tilde{A}_2 = \frac{\sqrt{3}}{5} v_{126}^2$, up to an overall factor.

References

- [1] P. A. R. Ade *et al.* [Planck Collaboration], arXiv:1502.01589 [astro-ph.CO].
- [2] H. Goldberg, Phys. Rev. Lett. **50** (1983) 1419; J. Ellis, J.S. Hagelin, D.V. Nanopoulos, K.A. Olive and M. Srednicki, Nucl. Phys. **B238** (1984) 453.
- [3] T. Appelquist, H. C. Cheng and B. A. Dobrescu, Phys. Rev. D **64**, 035002 (2001) [hep-ph/0012100]; H. C. Cheng, K. T. Matchev and M. Schmaltz, Phys. Rev. D **66**, 036005 (2002) [hep-ph/0204342]; G. Servant and T. M. P. Tait, Nucl. Phys. B **650**, 391 (2003) [hep-ph/0206071]; H. C. Cheng, J. L. Feng and K. T. Matchev, Phys. Rev. Lett. **89**, 211301 (2002) [hep-ph/0207125]; M. Kakizaki, S. Matsumoto and M. Senami, Phys. Rev. D **74**, 023504 (2006) [hep-ph/0605280]; G. Belanger, M. Kakizaki and A. Pukhov, JCAP **1102**, 009 (2011) [arXiv:1012.2577 [hep-ph]].
- [4] N. Arkani-Hamed, A. G. Cohen and H. Georgi, Phys. Lett. B **513**, 232 (2001) [hep-ph/0105239]; N. Arkani-Hamed, A. G. Cohen, E. Katz, A. E. Nelson, T. Gregoire and J. G. Wacker, JHEP **0208**, 021 (2002) [hep-ph/0206020]; N. Arkani-Hamed, A. G. Cohen, E. Katz and A. E. Nelson, JHEP **0207**, 034 (2002) [hep-ph/0206021]; H. C. Cheng and I. Low, JHEP **0408**, 061 (2004) [hep-ph/0405243]; I. Low, JHEP **0410**, 067 (2004) [hep-ph/0409025]; J. Hubisz and P. Meade, Phys. Rev. D **71**, 035016 (2005) [hep-ph/0411264]; A. Birkedal, A. Noble, M. Perelstein and A. Spray, Phys. Rev. D **74**, 035002 (2006) [hep-ph/0603077].
- [5] T. W. B. Kibble, G. Lazarides and Q. Shafi, Phys. Lett. B **113**, 237 (1982).
- [6] L. M. Krauss and F. Wilczek, Phys. Rev. Lett. **62**, 1221 (1989).
- [7] L. E. Ibanez and G. G. Ross, Phys. Lett. B **260**, 291 (1991); L. E. Ibanez and G. G. Ross, Nucl. Phys. B **368**, 3 (1992).
- [8] S. P. Martin, Phys. Rev. D **46**, 2769 (1992) [hep-ph/9207218].
- [9] M. Kadastik, K. Kannike and M. Raidal, Phys. Rev. D **81**, 015002 (2010) [arXiv:0903.2475 [hep-ph]]; M. Kadastik, K. Kannike and M. Raidal, Phys. Rev. D **80**, 085020 (2009) [Erratum-ibid. D **81**, 029903 (2010)] [arXiv:0907.1894 [hep-ph]].
- [10] M. Frigerio and T. Hambye, Phys. Rev. D **81**, 075002 (2010) [arXiv:0912.1545 [hep-ph]]; T. Hambye, PoS IDM **2010**, 098 (2011) [arXiv:1012.4587 [hep-ph]].
- [11] H. Georgi, AIP Conf. Proc. **23**, 575 (1975); H. Fritzsch and P. Minkowski, Annals Phys. **93**, 193 (1975).
- [12] M. S. Chanowitz, J. R. Ellis and M. K. Gaillard, Nucl. Phys. B **128**, 506 (1977); H. Georgi and D. V. Nanopoulos, Nucl. Phys. B **155**, 52 (1979).
- [13] H. Georgi and D. V. Nanopoulos, Nucl. Phys. B **159**, 16 (1979); C. E. Vayonakis, Phys. Lett. B **82**, 224 (1979) [Phys. Lett. **83B**, 421 (1979)].

- [14] A. Masiero, Phys. Lett. B **93**, 295 (1980).
- [15] Q. Shafi, M. Sondermann and C. Wetterich, Phys. Lett. B **92**, 304 (1980).
- [16] F. del Aguila and L. E. Ibanez, Nucl. Phys. B **177**, 60 (1981).
- [17] R. N. Mohapatra and G. Senjanovic, Phys. Rev. D **27**, 1601 (1983).
- [18] S. Rajpoot, Phys. Rev. D **22**, 2244 (1980); M. Yasue, Prog. Theor. Phys. **65**, 708 (1981) [Erratum-ibid. **65**, 1480 (1981)]; J. M. Gipson and R. E. Marshak, Phys. Rev. D **31**, 1705 (1985); D. Chang, R. N. Mohapatra, J. Gipson, R. E. Marshak and M. K. Parida, Phys. Rev. D **31**, 1718 (1985); N. G. Deshpande, E. Keith and P. B. Pal, Phys. Rev. D **46**, 2261 (1993); N. G. Deshpande, E. Keith and P. B. Pal, Phys. Rev. D **47**, 2892 (1993) [hep-ph/9211232]; S. Bertolini, L. Di Luzio and M. Malinsky, Phys. Rev. D **81**, 035015 (2010) [arXiv:0912.1796 [hep-ph]].
- [19] M. Fukugita and T. Yanagida, In *Fukugita, M. (ed.), Suzuki, A. (ed.): Physics and astrophysics of neutrinos* 1-248. and Kyoto Univ. - YITP-K-1050 (93/12,rec.Feb.94) 248 p. C.
- [20] L. Di Luzio, arXiv:1110.3210 [hep-ph].
- [21] G. Lazarides, Q. Shafi and C. Wetterich, Nucl. Phys. B **181**, 287 (1981).
- [22] P. Minkowski, Phys. Lett. B **67**, 421 (1977); T. Yanagida, Conf. Proc. C **7902131**, 95 (1979); M. Gell-Mann, P. Ramond and R. Slansky, Conf. Proc. C **790927**, 315 (1979) [arXiv:1306.4669 [hep-th]]; S. L. Glashow, NATO Sci. Ser. B **59**, 687 (1980); R. N. Mohapatra and G. Senjanovic, Phys. Rev. Lett. **44**, 912 (1980); R. N. Mohapatra and G. Senjanovic, Phys. Rev. D **23**, 165 (1981).
- [23] M. De Montigny and M. Masip, Phys. Rev. D **49**, 3734 (1994) [hep-ph/9309312].
- [24] Y. Mambrini, N. Nagata, K. A. Olive, J. Quevillon and J. Zheng, Phys. Rev. D **91**, 095010 (2015) [arXiv:1502.06929 [hep-ph]].
- [25] Y. Mambrini, K. A. Olive, J. Quevillon and B. Zaldivar, Phys. Rev. Lett. **110**, 241306 (2013) [arXiv:1302.4438 [hep-ph]].
- [26] K. S. Babu and S. Khan, arXiv:1507.06712 [hep-ph].
- [27] B. Bajc, A. Melfo, G. Senjanovic and F. Vissani, Phys. Rev. D **73**, 055001 (2006) [hep-ph/0510139].
- [28] T. Fukuyama, A. Ilakovac, T. Kikuchi, S. Meljanac and N. Okada, Eur. Phys. J. C **42**, 191 (2005) [hep-ph/0401213].
- [29] A. Masiero, D. V. Nanopoulos, K. Tamvakis and T. Yanagida, Phys. Lett. B **115**, 380 (1982); B. Grinstein, Nucl. Phys. B **206**, 387 (1982).

- [30] S. Dimopoulos and F. Wilczek, Print-81-0600 (SANTA BARBARA), NSF-ITP-82-07.
- [31] K. Inoue, A. Kakuto and H. Takano, Prog. Theor. Phys. **75**, 664 (1986); A. A. Anselm and A. A. Johansen, Phys. Lett. B **200**, 331 (1988).
- [32] G. R. Farrar and P. Fayet, Phys. Lett. B **76**, 575 (1978); S. Dimopoulos and H. Georgi, Nucl. Phys. B **193**, 150 (1981); S. Weinberg, Phys. Rev. D **26**, 287 (1982); N. Sakai and T. Yanagida, Nucl. Phys. B **197**, 533 (1982); S. Dimopoulos, S. Raby and F. Wilczek, Phys. Lett. B **112**, 133 (1982).
- [33] V. A. Kuzmin and M. E. Shaposhnikov, Phys. Lett. B **92**, 115 (1980); T. W. B. Kibble, G. Lazarides and Q. Shafi, Phys. Rev. D **26**, 435 (1982); D. Chang, R. N. Mohapatra and M. K. Parida, Phys. Rev. Lett. **52**, 1072 (1984); D. Chang, R. N. Mohapatra and M. K. Parida, Phys. Rev. D **30**, 1052 (1984); D. Chang, R. N. Mohapatra, J. Gipson, R. E. Marshak and M. K. Parida, Phys. Rev. D **31**, 1718 (1985).
- [34] I. Antoniadis, J. R. Ellis, J. S. Hagelin and D. V. Nanopoulos, Phys. Lett. B **194**, 231 (1987).
- [35] I. Antoniadis, J. R. Ellis, J. S. Hagelin and D. V. Nanopoulos, Phys. Lett. B **208**, 209 (1988) [Addendum-ibid. B **213**, 562 (1988)]; J. R. Ellis, J. L. Lopez and D. V. Nanopoulos, Phys. Lett. B **292**, 189 (1992) [hep-ph/9207237]; J. R. Ellis, D. V. Nanopoulos and K. A. Olive, Phys. Lett. B **300** (1993) 121 [hep-ph/9211325]; J. R. Ellis, J. L. Lopez, D. V. Nanopoulos and K. A. Olive, Phys. Lett. B **308**, 70 (1993) [hep-ph/9303307].
- [36] R. Slansky, Phys. Rept. **79**, 1 (1981).
- [37] M. Cirelli, N. Fornengo and A. Strumia, Nucl. Phys. B **753**, 178 (2006) [hep-ph/0512090]; M. Cirelli, A. Strumia and M. Tamburini, Nucl. Phys. B **787**, 152 (2007) [arXiv:0706.4071 [hep-ph]]; M. Cirelli and A. Strumia, New J. Phys. **11**, 105005 (2009) [arXiv:0903.3381 [hep-ph]].
- [38] R. Essig, Phys. Rev. D **78**, 015004 (2008) [arXiv:0710.1668 [hep-ph]].
- [39] T. Hambye, F.-S. Ling, L. Lopez Honorez and J. Rocher, JHEP **0907**, 090 (2009) [Erratum-ibid. **1005**, 066 (2010)].
- [40] J. Hisano, D. Kobayashi, N. Mori and E. Senaha, Phys. Lett. B **742**, 80 (2015) [arXiv:1410.3569 [hep-ph]].
- [41] N. Nagata and S. Shirai, JHEP **1501**, 029 (2015) [arXiv:1410.4549 [hep-ph]].
- [42] N. Nagata and S. Shirai, Phys. Rev. D **91**, 055035 (2015) [arXiv:1411.0752 [hep-ph]].
- [43] S. M. Boucenna, M. B. Krauss and E. Nardi, Phys. Lett. B **748**, 191 (2015) [arXiv:1503.01119 [hep-ph]].

- [44] K. Harigaya, K. Ichikawa, A. Kundu, S. Matsumoto and S. Shirai, arXiv:1504.03402 [hep-ph].
- [45] J. Heeck and S. Patra, arXiv:1507.01584 [hep-ph].
- [46] M. Cirelli, T. Hambye, P. Panci, F. Sala and M. Taoso, arXiv:1507.05519 [hep-ph]; C. Garcia-Cely, A. Ibarra, A. S. Lamperstorfer and M. H. G. Tytgat, arXiv:1507.05536 [hep-ph].
- [47] C. W. Chiang and E. Senaha, arXiv:1508.02891 [hep-ph].
- [48] B. Feldstein, M. Ibe and T. T. Yanagida, Phys. Rev. Lett. **112**, 101301 (2014) [arXiv:1310.7495 [hep-ph]].
- [49] V. Silveira and A. Zee, Phys. Lett. B **161**, 136 (1985); J. McDonald, Phys. Rev. D **50**, 3637 (1994) [hep-ph/0702143]; C. P. Burgess, M. Pospelov and T. ter Veldhuis, Nucl. Phys. B **619**, 709 (2001) [hep-ph/0011335]; H. Davoudiasl, R. Kitano, T. Li and H. Murayama, Phys. Lett. B **609**, 117 (2005) [hep-ph/0405097].
- [50] N. G. Deshpande and E. Ma, Phys. Rev. D **18**, 2574 (1978); E. Ma, Phys. Rev. D **73**, 077301 (2006) [hep-ph/0601225]; R. Barbieri, L. J. Hall and V. S. Rychkov, Phys. Rev. D **74**, 015007 (2006) [hep-ph/0603188]; L. Lopez Honorez, E. Nezri, J. F. Oliver and M. H. G. Tytgat, JCAP **0702**, 028 (2007) [hep-ph/0612275].
- [51] A. Arhrib, Y. L. S. Tsai, Q. Yuan and T. C. Yuan, JCAP **1406**, 030 (2014) [arXiv:1310.0358 [hep-ph]]; A. Ilnicka, M. Krawczyk and T. Robens, arXiv:1508.01671 [hep-ph].
- [52] T. W. Kephart and T. C. Yuan, arXiv:1508.00673 [hep-ph].
- [53] M. Farina, D. Pappadopulo and A. Strumia, JHEP **1308**, 022 (2013) [arXiv:1303.7244 [hep-ph]].
- [54] J. Hisano, S. Matsumoto and M. M. Nojiri, Phys. Rev. Lett. **92**, 031303 (2004) [hep-ph/0307216]; J. Hisano, S. Matsumoto, M. M. Nojiri and O. Saito, Phys. Rev. D **71**, 063528 (2005) [hep-ph/0412403].
- [55] M. Shiozawa, talk presented at TAUP 2013, September 8–13, Asilomar, CA, USA.
- [56] K. S. Babu, E. Kearns, U. Al-Binni, S. Banerjee, D. V. Baxter, Z. Berezhiani, M. Bergevin and S. Bhattacharya *et al.*, arXiv:1311.5285 [hep-ph].
- [57] J. M. Cline, K. Kainulainen, P. Scott and C. Weniger, Phys. Rev. D **88**, 055025 (2013) [arXiv:1306.4710 [hep-ph]]; M. Duerr, P. Fileviez Perez and J. Smirnov, arXiv:1508.04418 [hep-ph].
- [58] T. Abe, R. Kitano and R. Sato, Phys. Rev. D **91**, no. 9, 095004 (2015) [arXiv:1411.1335 [hep-ph]].

- [59] D. S. Akerib *et al.* [LUX Collaboration], Phys. Rev. Lett. **112**, 091303 (2014) [arXiv:1310.8214 [astro-ph.CO]].
- [60] G. Belanger, B. Dumont, U. Ellwanger, J. F. Gunion and S. Kraml, Phys. Rev. D **88**, 075008 (2013) [arXiv:1306.2941 [hep-ph]].
- [61] T. Abe and R. Sato, JHEP **1503**, 109 (2015) [arXiv:1501.04161 [hep-ph]].
- [62] J. Hisano, S. Matsumoto, M. Nagai, O. Saito and M. Senami, Phys. Lett. B **646**, 34 (2007) [hep-ph/0610249].
- [63] G. Lazarides, Q. Shafi and C. Wetterich, Nucl. Phys. B **181**, 287 (1981); K. S. Babu and R. N. Mohapatra, Phys. Rev. Lett. **70**, 2845 (1993) [hep-ph/9209215]; K. Matsuda, Y. Koide and T. Fukuyama, Phys. Rev. D **64**, 053015 (2001) [hep-ph/0010026]; T. Fukuyama, K. Ichikawa and Y. Mimura, arXiv:1508.07078 [hep-ph].
- [64] V. Khachatryan *et al.* [CMS Collaboration], JHEP **1504**, 025 (2015) [arXiv:1412.6302 [hep-ex]]; G. Aad *et al.* [ATLAS Collaboration], Phys. Rev. D **90**, no. 5, 052005 (2014) [arXiv:1405.4123 [hep-ex]].
- [65] G. Aad *et al.* [ATLAS Collaboration], arXiv:1508.04735 [hep-ex]; CMS Collaboration [CMS Collaboration], CMS-PAS-EXO-12-041; [CMS Collaboration], CMS-PAS-EXO-12-042.
- [66] M. Ibe, S. Matsumoto and R. Sato, Phys. Lett. B **721**, 252 (2013) [arXiv:1212.5989 [hep-ph]].
- [67] G. Aad *et al.* [ATLAS Collaboration], Phys. Rev. D **88**, 112006 (2013) [arXiv:1310.3675 [hep-ex]].
- [68] K. Shingo, CERN-THESIS-2014-163; M. Low and L. T. Wang, JHEP **1408**, 161 (2014) [arXiv:1404.0682 [hep-ph]]; M. Cirelli, F. Sala and M. Taoso, JHEP **1410**, 033 (2014) [Erratum-ibid. **1501**, 041 (2015)] [arXiv:1407.7058 [hep-ph]].
- [69] A. Kounine, talk presented at “AMS DAYS AT CERN—The Future of Cosmic Ray Physics and Latest Results”, April 15–17, 2015, CERN.
- [70] M. Ibe, S. Matsumoto, S. Shirai and T. T. Yanagida, Phys. Rev. D **91**, no. 11, 111701 (2015) [arXiv:1504.05554 [hep-ph]]; K. Hamaguchi, T. Moroi and K. Nakayama, Phys. Lett. B **747**, 523 (2015) [arXiv:1504.05937 [hep-ph]].
- [71] T. Cohen, M. Lisanti, A. Pierce and T. R. Slatyer, JCAP **1310**, 061 (2013) [arXiv:1307.4082]; J. Fan and M. Reece, JHEP **1310**, 124 (2013) [arXiv:1307.4400]; A. Hryczuk, I. Cholis, R. Iengo, M. Tavakoli and P. Ullio, JCAP **1407**, 031 (2014) [arXiv:1401.6212 [astro-ph.HE]].
- [72] A. Abramowski *et al.* [H.E.S.S. Collaboration], Phys. Rev. Lett. **110**, 041301 (2013) [arXiv:1301.1173].

- [73] M. Ackermann *et al.* [Fermi-LAT Collaboration], Phys. Rev. D **89**, 042001 (2014) [arXiv:1310.0828 [astro-ph.HE]].
- [74] B. Bhattacharjee, M. Ibe, K. Ichikawa, S. Matsumoto and K. Nishiyama, JHEP **1407**, 080 (2014) [arXiv:1405.4914 [hep-ph]].
- [75] J. Hisano, S. Matsumoto, M. M. Nojiri and O. Saito, Phys. Rev. D **71**, 015007 (2005) [hep-ph/0407168]; J. Hisano, K. Ishiwata and N. Nagata, Phys. Lett. B **690**, 311 (2010) [arXiv:1004.4090 [hep-ph]]; J. Hisano, K. Ishiwata and N. Nagata, Phys. Rev. D **82**, 115007 (2010) [arXiv:1007.2601 [hep-ph]]; J. Hisano, K. Ishiwata, N. Nagata and T. Takesako, JHEP **1107**, 005 (2011) [arXiv:1104.0228 [hep-ph]].
- [76] J. Hisano, K. Ishiwata and N. Nagata, JHEP **1506**, 097 (2015) [arXiv:1504.00915 [hep-ph]].
- [77] J. Billard, L. Strigari and E. Figueroa-Feliciano, Phys. Rev. D **89**, no. 2, 023524 (2014) [arXiv:1307.5458 [hep-ph]].
- [78] R. J. Hill and M. P. Solon, Phys. Lett. B **707**, 539 (2012) [arXiv:1111.0016 [hep-ph]]; R. J. Hill and M. P. Solon, Phys. Rev. Lett. **112**, 211602 (2014) [arXiv:1309.4092 [hep-ph]]; R. J. Hill and M. P. Solon, Phys. Rev. D **91**, 043504 (2015) [arXiv:1401.3339 [hep-ph]]; R. J. Hill and M. P. Solon, Phys. Rev. D **91**, 043505 (2015) [arXiv:1409.8290 [hep-ph]].
- [79] H. Baer, V. Barger, D. Mickelson, A. Mustafayev and X. Tata, JHEP **1406**, 172 (2014) [arXiv:1404.7510 [hep-ph]].
- [80] M. Fukugita and T. Yanagida, Phys. Lett. B **174**, 45 (1986).
- [81] F. Lemire and J. Patera, J. Math. Phys. **21**, 2026 (1980).
- [82] M. Machacek, Nucl. Phys. B **159**, 37 (1979).
- [83] S. Weinberg, Phys. Rev. Lett. **43**, 1566 (1979).
- [84] F. Wilczek and A. Zee, Phys. Rev. Lett. **43**, 1571 (1979).
- [85] L. F. Abbott and M. B. Wise, Phys. Rev. D **22**, 2208 (1980).
- [86] T. Nihei and J. Arafune, Prog. Theor. Phys. **93**, 665 (1995) [hep-ph/9412325].
- [87] Y. Aoki, E. Shintani and A. Soni, Phys. Rev. D **89**, 014505 (2014) [arXiv:1304.7424 [hep-lat]].
- [88] P. Fileviez Perez, Phys. Lett. B **595**, 476 (2004) [hep-ph/0403286].
- [89] C. Munoz, Phys. Lett. B **177**, 55 (1986).
- [90] W. E. Caswell, J. Milutinovic and G. Senjanovic, Phys. Rev. D **26**, 161 (1982).

- [91] P. Nath and R. M. Syed, Nucl. Phys. B **618**, 138 (2001) [hep-th/0109116];
T. Fukuyama, A. Ilakovac, T. Kikuchi, S. Meljanac and N. Okada, J. Math. Phys. **46**, 033505 (2005) [hep-ph/0405300].